

Multiple-impurity Anderson model for quantum dots coupled in parallelR. Žitko¹ and J. Bonča^{1,2}¹*Jožef Stefan Institute, Ljubljana, Slovenia*²*Faculty of Mathematics and Physics, University of Ljubljana, Ljubljana, Slovenia*

(Received 18 April 2006; revised manuscript received 30 May 2006; published 17 July 2006)

The system of several (N) quantum dots coupled in parallel to the same single-mode conduction channel can be modeled as a single-channel N -impurity Anderson model. Using the generalized Schrieffer-Wolff transformation we show that near the particle-hole symmetric point, the effective Hamiltonian in the local moment regime is the N -impurity $S=1/2$ Kondo model. The conduction-band-mediated RKKY exchange interaction between the dots is ferromagnetic and at intermediate temperatures locks the moments into a maximal spin $S=N/2$ ground state. We provide an analytical estimate for the RKKY interaction. At low temperatures the spin is partially screened by the conduction electrons to $N/2-1/2$ due to the Kondo effect. By comparing accurate numerical renormalization group results for magnetic susceptibility of the N -impurity Anderson model to the exact Bethe ansatz results of a $S=N/2$ SU(2) Kondo system we show that at low-temperature the quantum dots can be described by the effective $S=N/2$ Kondo model. Moreover, the Kondo temperature is independent of the number of impurities N . We demonstrate the robustness of the spin $N/2$ ground state as well as of the associated $S=N/2$ Kondo effect by studying the stability of the system with respect to various experimentally relevant perturbations. We finally explore various quantum phase transitions driven by these perturbations.

DOI: [10.1103/PhysRevB.74.045312](https://doi.org/10.1103/PhysRevB.74.045312)

PACS number(s): 73.63.Kv, 72.15.Qm, 73.23.Hk, 71.10.Hf

I. INTRODUCTION

The Kondo effect emerges as the increased scattering rate of the conduction band electrons at low temperatures due to the presence of magnetic impurities which induce spin-flip scattering. It leads to various anomalies in the thermodynamic and transport properties of the Kondo systems. It is usually described using simplified quantum impurity models such as the Kondo model and the Anderson model.¹ The quantum impurity models attract the interest of the solid-state physics community both due to their unexpectedly complex behavior and intrinsic beauty, as well as due to their ubiquitous applicability to a vast array of physical systems such as bulk Kondo systems, heavy-fermion compounds and other strongly correlated systems,² dissipative two-level systems,³ single magnetic impurities, and quantum dots.⁴⁻⁶

After the properties of single-impurity models were unraveled using a complementary set of techniques (the scaling approach, Wilson's numerical renormalization group, Bethe ansatz solution, and various large- N expansion schemes),² the attention has increasingly focused to multiple-impurity models. Research in this field has recently increased due to a multitude of experimental results made possible by advances in micro- and nanotechnology. The multiple-impurity magnetic nanostructures under study are predominantly of two kinds: clusters of magnetic adsorbates on surfaces of noble metals (Ni dimers,⁷ Ce trimers,⁸ molecular complexes⁹) and systems of multiple quantum dots.¹⁰⁻¹⁴

The most important additional element that emerges in multiple-impurity models is the Ruderman-Kittel-Kasuya-Yosida (RKKY) exchange interaction.¹⁵ It arises when the magnetic moments on the impurities induce spin polarization in the conduction band which leads to magnetic coupling of moments that are separated in space. The RKKY interaction depends on the interimpurity distance and can be either ferromagnetic or antiferromagnetic.

The competition between the antiferromagnetic RKKY interaction and the Kondo effect in two magnetically coupled local moments leads to a quantum phase transition at $J \sim T_K$ between strongly bound local magnetic singlet for $J \gg T_K$ and two separate Kondo singlets for $J \ll T_K$.¹⁶⁻²⁰ The role of the antiferromagnetic exchange interaction was also studied in the context of double quantum dots (DQD).²¹⁻²⁵ Two mechanisms can contribute to the effective exchange interaction between the dots: the conduction-band mediated RKKY interaction and the superexchange mechanism due to interdot electron hopping. Depending on the setup (serial or parallel embedding of the dots between the source and drain leads), either or both mechanisms may be significant. In magnetically coupled dots, embedded between the leads in series, the conductance is low for small exchange coupling when the Kondo singlets are formed between each dot and adjacent lead. Conductance is also low for large exchange coupling, when a local singlet state forms between the moments on the dots. In contrast, the conductance reaches the unitary limiting value of $2e^2/h$ in a narrow interval of J , such that $J \sim T_K$.^{21,22} The introduction of additional electron hopping between dots breaks the quantum critical transition, nevertheless, some signatures of the quantum phase transition remain detectable.²²

Strong ferromagnetic RKKY interaction between two magnetic impurities coupled to two conduction channels leads to three different regimes. At temperatures comparable to RKKY interaction, ferromagnetic locking of impurity spins occurs; this is followed by a two-stage freezing out of their local moment as they become screened by the conduction electrons.²⁶ This scenario was corroborated by numerical studies of the two-impurity Kondo model²⁷ and the Alexander-Anderson model.²⁸ Antiferromagnetic and ferromagnetic RKKY interactions lead to different transport properties of DQD systems.^{29,30} Due to recent advances in nanotechnology, the effects of RKKY interaction on transport properties became directly observable.¹³ Conductance

through Aharonov-Bohm (AB) interferometers with embedded quantum dots also depends on the RKKY interactions, which in turn depends on the magnetic flux.^{31–33} A similar system of two quantum dots, side-coupled to a single-mode channel, allows one to study the crossover between fully screened and underscreened Kondo impurity.³⁴

The physics of RKKY interactions is also related to the studies of the Kondo effect in integer-spin quantum dots.³⁵ By tuning the magnetic field, the energy difference between singlet and triplet spin states can be tuned to zero. At the degeneracy point, a large zero-bias resonance with an increased Kondo temperature is observed,³⁵ which can be understood in the framework of a two-orbital Anderson model.³⁶

The interplay of the Kondo effect and the interimpurity exchange interaction leads to a number of interesting phenomena observed in different realizations of the double quantum dot systems. For this reason, we present in this work a study of more general N quantum dot systems. Using the numerical renormalization group (NRG) technique as our primary tool and various analytical approaches we investigate the effects of the RKKY interaction in a multiple-impurity Anderson model. We present results of thermodynamic properties, in particular the impurity contribution to the magnetic susceptibility and the entropy, as well as various correlation functions. This work also provides a setting for further studies of transport properties of this class of systems.

The paper is organized as follows. In Sec. II we describe the class of models under study as well as model parameters and approximations used in this work. In Sec. III we describe the existence of a hierarchy of separated time (and energy) scales and we introduce effective models valid at different temperatures. In Sec. IV we describe the numerical methods that are used in Sec. V to study the multiple-impurity Anderson models. Finally, in Sec. VI we test the stability of the $S=1$ state in the two impurity model with respect to various perturbation. Tedious derivations of scaling equations and perturbation theory approaches are given in the appendixes.

II. THE MODEL

We study models of N impurities coupled to one single-mode conduction channel. The motivation for such models comes primarily from experiments performed on systems of several quantum dots connected in parallel between source and drain electron reservoirs. Since quantum dots can be made to behave as single magnetic impurities, such systems can be modeled in the first approximation as several Anderson impurities embedded between two tight-binding lattices as shown schematically in Fig. 1. If the coupling to the left and right electrode of each quantum dot is symmetric, it can be shown that each dot couples only to the symmetric combination of conduction electron wave functions from left and right lead, while the antisymmetric combinations of wave functions are totally decoupled and are irrelevant for our purpose.³⁷ We can thus model the parallel quantum dots using the following simplified Hamiltonian, which we name the “ N -impurity Anderson model:”

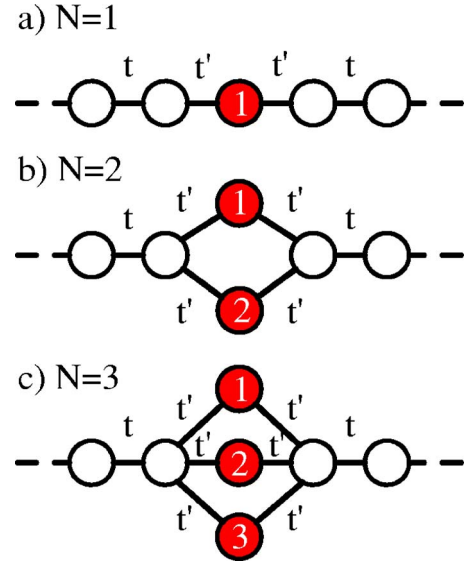


FIG. 1. (Color online) Systems of parallel quantum dots. The tight-binding hopping parameter t determines the half-width of the conduction band, $D=2t$, while parameter t' is related to the hybridization Γ by $\Gamma/D=(t'/t)^2$.

$$H = H_{\text{band}} + H_{\text{dots}} + H_c. \quad (1)$$

Here $H_{\text{band}} = \sum_{k\sigma} \epsilon_k c_{k\sigma}^\dagger c_{k\sigma}$ is the conduction band Hamiltonian. $H_{\text{dots}} = \sum_{i=1}^N H_{\text{dot},i}$ with

$$H_{\text{dot},i} = \delta(n_i - 1) + \frac{U}{2}(n_i - 1)^2 = \epsilon_d n_i + U n_{\uparrow i} n_{\downarrow i} \quad (2)$$

is the quantum dot Hamiltonian. Finally,

$$H_c = \frac{1}{\sqrt{L}} \sum_{k\sigma i} (V_k d_{i\sigma}^\dagger c_{k\sigma} + \text{H.c.}) \quad (3)$$

is the coupling Hamiltonian, where L is a normalization constant. The number operator n_i is defined as $n_i = \sum_{\sigma} d_{i\sigma}^\dagger d_{i\sigma}$. Parameter δ is related to the more conventional on-site energy ϵ_d by $\delta = \epsilon_d + U/2$, where U is the on-site Coulomb electron-electron ($e-e$) repulsion. For $\delta=0$ the model is particle-hole symmetric under the transformation $c_{k\sigma}^\dagger \rightarrow c_{k,-\sigma}$, $d_{i\sigma}^\dagger \rightarrow -d_{i,-\sigma}$. Parameter δ thus represents the measure for the departure from the particle-hole symmetric point.

To cast the model into a form that is more convenient for a numerical renormalization group study, we make two more approximations. We first linearize the dispersion relation ϵ_k of the conduction band, which gives $\epsilon_k = Dk$. The wave number k runs from -1 to 1 , therefore $2D$ is the width of the conduction band. This assumption is equivalent to adopting a constant density of states, $\rho_0 = 1/(2D)$. Second, we approximate the dot-band coupling with a constant hybridization strength, $\Gamma = \pi \rho_0 |V_{k_F}|^2$. Neither of these approximations affects the results in a significant way. In the rest of the paper, we will present results in terms of the parameters D and Γ , instead of the parameters t and t' of the original tight-binding models depicted in Fig. 1. Our notation follows that of Refs. 38 and 39 for easier comparison of the N -impurity results with the single-impurity case.

III. LOW-TEMPERATURE EFFECTIVE MODELS

Our primary goal is to demonstrate that the low-temperature effective model for the multiple impurity system is the $S=N/2$ SU(2) Kondo model:

$$H = H_{\text{band}} + \sum_{k'k} J_{k'k} \mathbf{s}_{kk'} \cdot \mathbf{S}, \quad (4)$$

where $\mathbf{s}_{kk'} = \frac{1}{2} \sum_{\alpha\alpha'} c_{k\alpha}^\dagger \boldsymbol{\sigma}_{\alpha\alpha'} c_{k'\alpha'}$ is the local-spin density in the Wannier orbital in the conduction band that couples to *all* N impurities. \mathbf{S} is the collective impurity $S=N/2$ spin operator and $J_{k'k}$ is the momentum-dependent antiferromagnetic spin-exchange interaction that can be derived using the Schrieffer-Wolff transformation. Results for $J_{k'k}$ are independent of N .

We first argue in favor of the validity of the effective Hamiltonian, proposed in Eq. (4), by considering the different time scales of the original N -impurity Anderson problem. To simplify the argument we further focus on the (nearly) symmetric case $\delta \ll U$ within the Kondo regime, $U/(\Gamma\pi) \gg 1$.

The shortest time scale, $\tau_U \sim \hbar/U$, represents charge excitations. The longest time scale is associated with the Kondo effect (magnetic excitations) and it is given by $\tau_K \sim \hbar/T_K$ where T_K is the Kondo temperature of the *single impurity Anderson model*, given by Haldane's expression

$$T_K = 0.182U \sqrt{\rho_0 J_K} \exp\left(-\frac{1}{\rho_0 J_K}\right), \quad (5)$$

where J_K is the effective antiferromagnetic Kondo exchange interaction and $\rho_0 J_K = 8\Gamma/\pi U$. This expression is valid for $U \ll D$ and $\delta=0$.

As we will show later, there is an additional time scale $\tau_J \sim \hbar/J_{\text{RKKY}}$, originating from the *ferromagnetic* RKKY dot-dot interactions:

$$J_{\text{RKKY}} \sim U(\rho_0 J_K)^2 = \frac{64 \Gamma^2}{\pi^2 U}. \quad (6)$$

From the condition for a well-developed Kondo effect, $U/(\Gamma\pi) \gg 1$, we obtain $J_{\text{RKKY}} \ll U$. We thus establish a hierarchy of time scales $\tau_U \ll \tau_J \ll \tau_K$.

Based on the three different time scales, we predict the existence of three distinct regimes close to the particle-hole symmetric point. The local moment regime is established at $T \sim T_1^*$, where $T_1^* = U/\alpha$ and α is a constant of the order one.³⁸ In this regime the system behaves as N independent spin $S=1/2$ impurities. At $T \sim T_F^*$, where $T_F^* = J_{\text{RKKY}}/\beta$ and β is a constant of the order one, spins bind into a high-spin $S=N/2$ state. With further lowering of the temperature, at $T \sim T_K$ the $S=N/2$ object experiences the Kondo effect which screens half a unit of spin (since there is a single conduction channel) to give a ground-state spin of $S-1/2=(N-1)/2$.

A. Schrieffer-Wolff transformation for multiple impurities

For $T < T_1^*$, the single impurity Anderson model can be mapped using the Schrieffer-Wolff transformation⁴⁰ to an s - d exchange model (the Kondo model) with an energy de-

pendent antiferromagnetic exchange interaction $J_{k'k}$. In this section we show that for multiple impurities a generalized Schrieffer-Wolff transformation can be performed and that below T_1^* , the N -impurity Anderson model maps to the N -impurity $S=1/2$ Kondo model. Furthermore, the exchange constant is shown to be the same as in the single impurity case.

Due to the hybridization term V_k , the electrons are hopping on and off the impurities. Since all impurities are coupled to the same Wannier orbital, it could be expected that these hopping transitions would somehow "interfere." It should be recalled, however, that the dwelling time τ_U is much shorter than the magnetic time scales τ_J and τ_K . In other words, spin-flips are realized on a much shorter time scale compared to the mean time between successive spin-flips; for this reason, each local moment may be considered as independent. Note that the impurities do in fact "interfere:" there are $O(V_k^4)$ processes which lead to an effective ferromagnetic RKKY exchange interaction between pairs of spins and ultimately to the ferromagnetic ordering of spins at temperatures below $\sim J_{\text{RKKY}}$. This will be discussed in the following section.

The Schrieffer-Wolff transformation is a canonical transformation that eliminates hybridization terms V_k to first order from the Hamiltonian H , i.e., it requires that⁴⁰

$$\bar{H} \equiv e^{\mathcal{S}} H e^{-\mathcal{S}} \quad (7)$$

have no terms which are first order in V_k . We expand \bar{H} in terms of nested commutators:

$$\bar{H} = H + [\mathcal{S}, H] + \frac{1}{2}[\mathcal{S}, [\mathcal{S}, H]] + \dots \quad (8)$$

and write $H = H_0 + H_c$, where $H_0 = H_{\text{band}} + H_{\text{dots}}$. We then choose \mathcal{S} to be first order in V_k so that

$$[\mathcal{S}, H_0] + H_c = 0. \quad (9)$$

As previously discussed, each impurity can be considered independent due to the separation of time scales. Therefore we choose the generator \mathcal{S} to be the sum $\mathcal{S} = \sum_i \mathcal{S}_i$ of generators \mathcal{S}_i , where the generator \mathcal{S}_i for each impurity has the same form as in the single-impurity case:

$$\mathcal{S}_i = \sum_{k\sigma\alpha} \frac{V_k}{\epsilon_k - \epsilon_\alpha} n_{i,-\sigma}^\alpha c_{k\sigma}^\dagger d_{i\sigma} - \text{H.c.} \quad (10)$$

with $\epsilon_\pm = \delta \pm U/2$ and the projection operators $n_{i,-\sigma}^\alpha$ are defined by

$$\begin{aligned} n_{i,-\sigma}^+ &= n_{i,-\sigma}, \\ n_{i,-\sigma}^- &= 1 - n_{i,-\sigma}. \end{aligned} \quad (11)$$

The resulting effective Hamiltonian is then given by

$$H_{\text{eff}} = H_0 + \frac{1}{2}[\mathcal{S}, H_c], \quad (12)$$

which features $O(V_k^2)$ effective interactions with the leading terms that can be cast in the form of the Kondo antiferromagnetic exchange interaction

$$H_{\text{ex}} = \sum_i \left(\sum_{kk'} J_{k'k} \mathbf{s}_{kk'} \cdot \mathbf{S}_i \right), \quad (13)$$

where \mathbf{S}_i is the $S=1/2$ spin operator on impurity i defined by $\mathbf{S}_i = \frac{1}{2} \sum_{\alpha\alpha'} d_{i\alpha}^\dagger \boldsymbol{\sigma} d_{i\alpha'}$ and the exchange constant $J_{k'k}$ is given by

$$J_{k'k} = V_{k'} V_k \left(\frac{1}{\epsilon_k - (\delta + U/2)} + \frac{1}{\epsilon_{k'} - (\delta + U/2)} - \frac{1}{\epsilon_k - (\delta - U/2)} - \frac{1}{\epsilon_{k'} - (\delta - U/2)} \right). \quad (14)$$

If we limit the wave vectors to the Fermi surface, i.e., for $k=k'=k_F$, we obtain

$$J_K \equiv 2|V_{k_F}|^2 \left(\frac{1}{|\delta - U/2|} + \frac{1}{|\delta + U/2|} \right). \quad (15)$$

This result is identical to $J_{k'k}$ obtained for a single impurity.⁴⁰

As it turns out, the Schrieffer-Wolff transformation, Eqs. (7)–(12), produces interimpurity interaction terms in addition to the expected impurity-band interaction terms. In the particle-hole symmetric case ($\delta=0$), these additional terms can be written as

$$\Delta H_{\text{eff}} = 2 \frac{|V_k|^2}{U} \left(\sum_{i=1}^N n_i - N \right) h_{\text{hop}}, \quad (16)$$

where

$$h_{\text{hop}} = \sum_{i<j,\sigma} (d_{i\sigma}^\dagger d_{j\sigma} + d_{j\sigma}^\dagger d_{i\sigma}). \quad (17)$$

Since the on-site charge repulsion favors states with single occupancy of each impurity, the term in the parenthesis in Eq. (16) is on the average equal to zero. Furthermore, if each site is singly occupied, possessing small fluctuations of the charge $\langle n_i^2 \rangle - \langle n_i \rangle^2 \sim 0$, hopping between the sites is suppressed and the term h_{hop} represents another small factor. The Hamiltonian ΔH is thus clearly not relevant: impurities are indeed independent.

On departure from the particle-hole symmetric point ($\delta \neq 0$), ΔH_{eff} generalizes to

$$\Delta H_{\text{eff}} = 2 \frac{U|V_k|^2}{U^2 - 4\delta^2} \left[\left(\sum_{i=1}^N n_i - N \right) - 2N \frac{\delta}{U} \right] h_{\text{hop}}. \quad (18)$$

For moderately large δ/U this Hamiltonian term still represents only a small correction to Eq. (13). However, for strong departure from the particle-hole (p-h) symmetric point, close to the valence-fluctuation regime (i.e., $\delta \rightarrow U/2$), the ΔH_{eff} becomes comparable in magnitude to H_{ex} and generates hopping of electrons between the impurities.

The above discussion leads us to the conclusion that just below T_1^* the effective Hamiltonian close to the p-h symmetric point is

$$H_{\text{eff}} = H_{\text{band}} + \sum_i \sum_{k'k} J_{k'k} \mathbf{s}_{kk'} \cdot \mathbf{S}_i. \quad (19)$$

If the dots are described by unequal Hamiltonians $H_{\text{dot},i}$ or have unequal hybridizations $V_{k'}^i$, then the mapping of the

multiple-impurity Anderson model to a multiple-impurity Kondo model still holds, however, with different effective exchange constants $J_{k'k}^i$.

B. RKKY interaction and ferromagnetic spin ordering

We now show that the effective RKKY exchange interaction between the spins in the effective N -impurity Kondo model, Eq. (19), is ferromagnetic and also responsible for locking of spins in a state of high total spin for temperatures below $T < J_{\text{RKKY}}$.

The ferromagnetic character of the RKKY interaction is expected, as shown by the following qualitative argument. We factor out the spin operators in the effective Hamiltonian Eq. (19):

$$H_{\text{eff}} = H_{\text{band}} + \left(\sum_{k'k} J_{k'k} \mathbf{s}_{kk'} \right) \cdot \sum_i \mathbf{S}_i. \quad (20)$$

Spins \mathbf{S}_i are aligned in the ground state since such orientation minimizes the energy of the system. This follows from considering a spin chain with N sites in a “static magnetic field” $\sum_{k'k} J_{k'k} \mathbf{s}_{kk'}$. The assumption of a static magnetic field is valid due to the separation of relevant time scales, $\tau_K \gg \tau_J$. States with $S < N/2$ are clearly excited states with one or several “misaligned” spins.

Since the interdot spin-spin coupling is a special case of the Ruderman-Kittel-Kasuya-Yosida (RKKY) interaction in bulk systems,¹⁵ a characteristic functional dependence given by

$$J_{\text{RKKY}} \propto U(\rho_0 J_K)^2 = \frac{64 \Gamma^2}{\pi^2 U} = \frac{16 V_{k_F}^4}{D^2 U} \quad (21)$$

is expected. The factor U in front of $(\rho_0 J_K)^2$ plays the role of a high-energy cutoff, much like the $0.182U$ effective-bandwidth factor in the expression for T_K , Eq. (5).

Using the Rayleigh-Schrödinger perturbation theory we calculated the singlet and triplet ground state energies E_S and E_T to the fourth order in V_k for the two-impurity case (see Appendix A). We define the RKKY exchange parameter by $J_{\text{RKKY}} = E_S - E_T$; positive value of J_{RKKY} corresponds to ferromagnetic RKKY interaction. For $U/D \leq 0.1$, the prefactor of $(\rho_0 J_K)^2$ in expression (21) is indeed found to be linear in U . Together with the prefactor the perturbation theory leads to

$$J_{\text{RKKY}} = 0.62 U (\rho_0 J_K)^2 \quad \text{for } U/D \ll 1, \quad (22)$$

which, as we will show later, fits very well our numerical results. The RKKY interaction becomes fully established for temperatures below T_J which is roughly one or two orders of magnitude smaller than T_1^* (T_J is defined in Appendix A). Since the RKKY interactions in the first approximation do not depend much on the number of impurities, for $N > 2$ the exchange interaction between each pair of impurities has the same strength as in the two impurity case. Therefore, for temperatures just below T_J , the effective Hamiltonian for the N -impurity Anderson model becomes

$$H_{\text{eff}} = H_{\text{band}} + \left(\sum_{k'k} J_{k'k} \mathbf{S}_{kk'} \right) \cdot \sum_i \mathbf{S}_i - J_{\text{RKKY}} \sum_{i<j} \mathbf{S}_i \cdot \mathbf{S}_j. \quad (23)$$

When the temperature drops below a certain temperature T_F^* , the spins align and form a ferromagnetically frozen state of maximum spin $S=N/2$. The transition temperature T_F^* is generally of the same order as J_{RKKY} , i.e., $T_F^* = J_{\text{RKKY}}/\beta$, where β is an N -dependent constant of the order one. This relation holds if $T_F^* \ll T_J$, otherwise T_F^* needs to be determined using a self-consistency equation (A5), as discussed in Appendix A.

In conclusion, for $T \leq T_F^*$ the states with total spin less than $N/2$ can be neglected, and the system behaves as if it consisted of a single spin \mathbf{S} of magnitude $S=N/2$. The effective Hamiltonian at very low temperatures is therefore the $S=N/2$ SU(2) Kondo model

$$H_{\text{eff}} = H_{\text{band}} + \sum_{k,k'} J_{k'k} \mathbf{S}_{k,k'} \cdot \mathbf{S}, \quad (24)$$

where $\mathbf{S} = \mathcal{P}(\sum_i \mathbf{S}_i) \mathcal{P}$ and \mathcal{P} is the projection operator on the subspace with total spin $S=N/2$. Other multiplets are irrelevant at temperatures below T_F^* . We point out that the Kondo temperature for this model is given by the formula for the single impurity Anderson model, Eq. (5), irrespective of the number of dots N , since the ferromagnetic interaction only leads to moment ordering, while the exchange interaction of the collective spin is still given by the same $J_{k'k}$.

It should be mentioned that if the exchange constants $J_{k'k}^i$ for different impurities are different, there will be some mixing between the spin multiplets. The simple description of impurities as a collective $S=N/2$ spin still holds even for relatively large differences, but in general the virtual excitations to other spin multiplets must be taken into account. This is studied in detail for the case of two dots in Sec. VI D.

IV. THE METHODS

A. Numerical renormalization group

The method of choice to study the low-temperature properties of quantum impurity models is the Wilson's numerical renormalization group (NRG).^{38,39,41} The NRG technique consists of logarithmic discretization of the conduction band described by H_{band} , mapping onto a one-dimensional chain with exponentially decreasing hopping constants, and iterative diagonalization of the resulting Hamiltonian. Since all N impurities couple to the band in the same manner, they all couple to the same, zeroth site of the chain Hamiltonian.³⁸

$$\begin{aligned} \frac{H_C}{D} &= \frac{1}{2}(1 + \Lambda^{-1}) \times \sum_{n=0}^{\infty} \sum_{\sigma} \Lambda^{-n/2} \xi_n [f_{n,\sigma}^{\dagger} f_{n+1,\sigma} + f_{n+1,\sigma}^{\dagger} f_{n,\sigma}] \\ &+ H_{\text{dots}} + \sum_{i,\sigma} \left(\frac{2\Gamma}{\pi D} \right)^{1/2} (f_{0\sigma}^{\dagger} d_{i\sigma} + d_{i\sigma}^{\dagger} f_{0\sigma}). \end{aligned} \quad (25)$$

Here $f_{n\sigma}^{\dagger}$ are the chain creation operators and ξ_n are constants of order 1. In addition to the conventional Wilson's discretization scheme,⁴¹ we also used Campo and Oliveira's new discretization approach using an overcomplete basis of

states⁴² with $\Lambda=4$, which improved convergence to the continuum limit. We made use of the “ z -trick” with typically six equally spaced values of the parameter z .⁴³

1. Symmetries

The Hamiltonian (1) has the following symmetries: (a) U(1)_{gauge} symmetry due to global phase (gauge) invariance. The corresponding conserved quantity is the total charge (defined with respect to half-filling case): $Q = \sum_i (n_i - 1)$, where the sum runs over all the impurity as well as the lead sites; (b) SU(2)_{spin} spin symmetry with generators $\mathbf{S} = \sum_{i\alpha} \frac{1}{2} \sum_{\alpha\alpha'} a_{i\alpha}^{\dagger} \boldsymbol{\sigma}_{\alpha\alpha'} a_{i\alpha'}$, where $\boldsymbol{\sigma}$ are the Pauli matrices. Since operators Q , \mathbf{S}^2 , and S_z commute with H , the invariant subspaces can be classified according to quantum numbers Q , S , and S_z . Computation of matrix elements can be further simplified using the Wigner-Eckart theorem.³⁸

In the particle-hole symmetric point, i.e., $\delta=0$, the Hamiltonian has an additional SU(2)_{iso} isospin symmetry.¹⁷ We define isospin operators on impurity site i using

$$\mathbf{I}_i = \sum_{\alpha\alpha'} \boldsymbol{\eta}_{i,\alpha}^{\dagger} \boldsymbol{\sigma}_{\alpha\alpha'} \boldsymbol{\eta}_{i,\alpha'}, \quad (26)$$

where the Nambu spinor $\boldsymbol{\eta}_i^{\dagger}$ on the impurity orbitals is defined by

$$\boldsymbol{\eta}_i^{\dagger} = \begin{pmatrix} d_{i,\uparrow}^{\dagger} \\ -d_{i,\downarrow} \end{pmatrix}. \quad (27)$$

We also define $I^+ = I^x + iI^y$ and $I^- = (I^+)^{\dagger}$. We then have, for example, $I_i^z = (n_i - 1)/2 = Q_i/2$ and $I_i^+ = d_{i,\downarrow}^{\dagger} d_{i,\uparrow}^{\dagger}$. The isospin symmetry is thus related to the electron pairing. In terms of the isospin operators the impurity Hamiltonian can be written as

$$H_{\text{dot},i} = 2\delta I_i^z + 4U(I_i^z)^2 = 2\delta I_i^z + \frac{4}{3}U(I_i)^2, \quad (28)$$

where we took into account that for spin-1/2 operators (Pauli matrices) $(I_i^z)^2 = 1/3(I_i)^2$.

On the Wilson chain the isospin is defined similarly but with a sign alternation in the definition of the Nambu spinors ξ_n :

$$\xi_n^{\dagger} = \begin{pmatrix} f_{n,\uparrow}^{\dagger} \\ (-1)^n f_{n,\downarrow} \end{pmatrix}. \quad (29)$$

The total isospin operator is obtained through a sum of \mathbf{I}_i for all orbitals of the problem (impurities and conduction band). For $\delta=0$, both \mathbf{I}^2 and I_z commute with H and I and I_z are additional good quantum numbers. Note that $I_z = Q/2$, therefore U(1)_{gauge} is in fact a subgroup of SU(2)_{iso}. Due to isotropy in isospin space, the I_z dependence can again be taken into account using the Wigner-Eckart theorem.

Spin and isospin operators commute, $[S_i, I_j] = 0$ for all i, j . Therefore for $\delta=0$ the problem has a SU(2)_{spin} \otimes SU(2)_{iso} symmetry which, when explicitly taken into account, leads to a further significant reduction of the numerical task.

In all our NRG calculations we took into account the conservation of the charge and the rotational invariance in the

spin space, i.e., the $U(1)_{\text{gauge}} \otimes SU(2)_{\text{spin}}$ symmetry which holds for all perturbed models considered, or the $SU(2)_{\text{spin}} \otimes SU(2)_{\text{isospin}}$ symmetry where applicable. The number of states that we kept in each stage of the NRG iteration depended on the number of the dots N , since the degeneracy increases exponentially with N : approximately as 4^N at the high-temperature free orbital regime and as 2^N in the local-moment regime. In the most demanding $N=4$ calculation we kept up to 12 000 states at each iteration (which corresponds to $>32\,000$ states taking into account the spin multiplicity of states), which gave fully converged results for the magnetic susceptibility.

For large scale NRG calculations it is worth taking into account that the calculation of eigenvalues scales as $O(n^2)$ and the calculation of eigenvectors as $O(n^3)$, where n is the dimension of the matrix being diagonalized. Since eigenvectors of the states that are truncated are not required to recalculate various matrices prior to performing a new iteration, a considerable amount of time can be saved by not calculating them at all.

2. Calculated quantities

We have computed the following thermodynamic quantities.

(1) The temperature-dependent impurity contribution to the magnetic susceptibility $\chi_{\text{imp}}(T)$

$$\chi_{\text{imp}}(T) = \frac{(g\mu_B)^2}{k_B T} (\langle S_z^2 \rangle - \langle S_z^2 \rangle_0), \quad (30)$$

where the subscript 0 refers to the situation when no impurities are present (i.e., H is simply the band Hamiltonian H_{band}), g is the electronic g factor, μ_B the Bohr magneton, and k_B the Boltzmann's constant. It should be noted that the combination $T\chi_{\text{imp}}/(g\mu_B)^2$ can be considered as an effective moment of the impurities, μ_{eff} .

(2) The temperature-dependent impurity contribution to the entropy $S_{\text{imp}}(T)$

$$S_{\text{imp}}(T) = \frac{(E-F)}{T} - \frac{(E-F)_0}{T}, \quad (31)$$

where $E = \langle H \rangle = \text{Tr}(H e^{-H/(k_B T)})$ and $F = -k_B T \ln \text{Tr}(e^{-H/(k_B T)})$. From the quantity S_{imp}/k_B we can deduce the effective degrees-of-freedom ν of the impurity as $S_{\text{imp}}/k_B \sim \ln \nu$.

(3) Thermodynamic expectation values of various operators such as the on-site occupancy $\langle n_i \rangle$, local charge fluctuations $\langle (\delta n)^2 \rangle = \langle n_i^2 \rangle - \langle n_i \rangle^2$, local-spin $\langle S_i^2 \rangle$, and spin-spin correlations $\langle S_i \cdot S_j \rangle$.

In the following we drop the subscript imp in χ_{imp} , but one should keep in mind that impurity contribution to the quantity is always implied. We also set $k_B=1$.

B. Bethe ansatz

The single-channel $SU(2)$ Kondo model can be exactly solved for an arbitrary spin of the impurity using the Bethe ansatz (BA) method.^{44–46} This technique gives exact results for thermodynamic quantities, such as magnetic susceptibil-

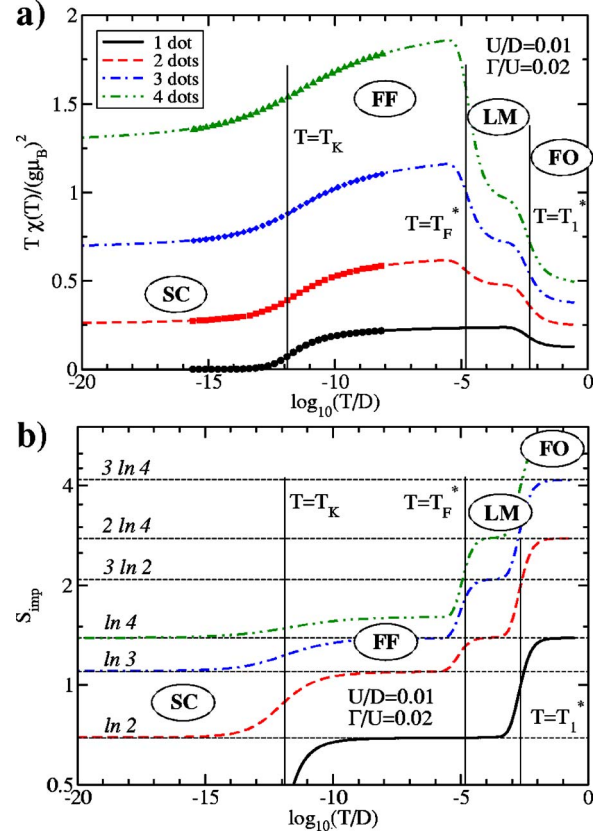


FIG. 2. (Color online) (a) Temperature-dependent susceptibility and (b) entropy of the N -dot systems calculated using the NRG. The symbols in the susceptibility plots were calculated using the thermodynamic Bethe ansatz approach for the corresponding $S=N/2$ $SU(2)$ Kondo models (\bullet : $S=1/2$, \blacksquare : $S=1$, \blacklozenge : $S=3/2$, and \blacktriangle : $S=2$).

ity, entropy, and heat capacity. It is, however, incapable of providing spectral and transport properties. For the purpose of comparing results of the single-channel $SU(2)$ Kondo model with NRG results of the N -impurity Anderson model, we have numerically solved the system of coupled integral equations using a discretization scheme as described, for example, in Ref. 46.

C. Scaling analysis

Certain aspects of the Kondo physics can be correctly captured using the perturbative renormalization group approach based on the “poor-man’s scaling” technique due to Anderson.⁴⁷ A brief account of this method is given in Appendix B.

V. NUMERICAL RESULTS

We choose the parameters U and Γ well within the Kondo regime, $U/(\Gamma\pi) \gg 1$. The relevant energy scales are then well separated ($T_K \ll T_F^* \ll T_I^*$) which enables clear identification of various regimes and facilitates analytical predictions (see also Sec. III).

In Fig. 2 we show temperature dependence of magnetic

TABLE I. Kondo temperatures for different numbers of quantum dots N corresponding to plots in Fig. 2.

N	Kondo temperature T_K/D	LM-FO temperature T_F^*/D
1	1.20×10^{-12}	
2	1.23×10^{-12}	1.87×10^{-5}
3	1.29×10^{-12}	2.11×10^{-5}
4	1.32×10^{-12}	2.32×10^{-5}

susceptibility and entropy for $N=1, 2, 3$, and 4 systems. As the temperature is reduced, the system goes through the following regimes.

(1) At high temperatures, $T > T_1^*$, the impurities are independent and they are in the *free orbital regime* (FO) (states $|0\rangle, |\uparrow\rangle, |\downarrow\rangle$, and $|2\rangle$ on each impurity are equiprobable). Each dot then contributes $1/8$ to $\mu_{\text{eff}} = T\chi/(g\mu_B)^2$ for a total of $\mu_{\text{eff}} = N/8$. The entropy approaches $S_{\text{imp}} = N \ln 4$ since all possible states are equally probable.³⁸

(2) For $T_F^* < T < T_1^*$ each dot is in the *local-moment regime* (LM) (states $|\uparrow\rangle$ and $|\downarrow\rangle$ are equiprobable, while the states $|0\rangle$ and $|2\rangle$ are suppressed). Each dot then contributes $1/4$ to μ_{eff} for a total of $N/4$. The entropy decreases to $S_{\text{imp}} = N \ln 2$.

(3) For $T_K < T < T_F^*$ and $N \geq 1$ the dots lock into a high spin state $S = N/2$ due to ferromagnetic RKKY coupling between local moments formed on the impurities. This is the *ferromagnetically frozen regime* (FF)²⁶ with $\mu_{\text{eff}} = S(S+1)/3 = N/2(N/2+1)/3$. The entropy decreases further to $S_{\text{imp}} = \ln(2S+1) = \ln(N+1)$.

(4) Finally, for $T < T_K$, the total spin is screened from $S = N/2$ to $\tilde{S} = S - 1/2 = (N-1)/2$ as we enter the partially quenched, Kondo screened *strong-coupling* (SC) N -impurity regime with $\mu_{\text{eff}} = \tilde{S}(\tilde{S}+1)/3 = (N-1)/2[(N-1)/2+1]/3$. The remaining $S - 1/2$ spin is a complicated object: a $S = N/2$ multiplet combination of the impurity spins antiferromagnetically coupled by a spin-1/2 cloud of the lead.²⁶ In this regime, the entropy reaches its minimum value of $S_{\text{imp}} = \ln(2\tilde{S}+1) = \ln N$.

In Fig. 2, atop the NRG results we additionally plot the results for the magnetic susceptibility of the $S = N/2$ SU(2) Kondo model obtained using an exact thermodynamic Bethe ansatz method (see Sec. IV B). For $T < T_F^*$ nearly perfect agreement between the N -impurity Anderson model and the corresponding $S = N/2$ SU(2) Kondo model are found over many orders of magnitude.⁷⁵ This agreement is used to extract the Kondo temperature of the multiple-impurity Anderson model. The fitting is performed numerically by the method of least-squares; in this manner very high accuracy of the extracted Kondo temperature can be achieved. The results in Table I point out the important result of this work that the Kondo temperature is nearly independent of N , as predicted in Sec. III B. In this sense, the locking of spins into a high-spin state does not, by itself, weaken the Kondo effect;^{13,30} however, it does modify the temperature dependence of the thermodynamic and transport properties.^{48,49}

It is instructive to follow transitions from the high-temperature FO regime to the LM and FF regimes through a

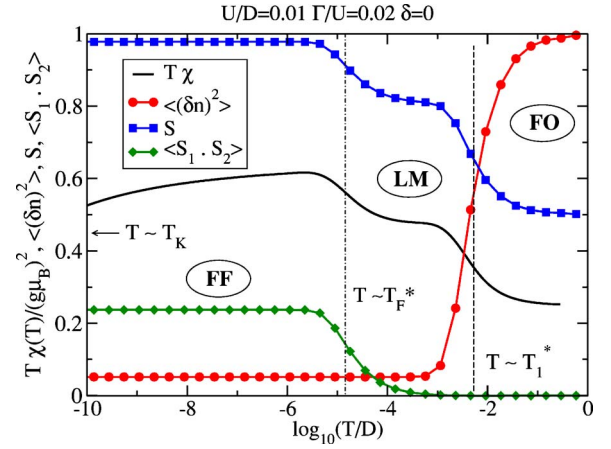


FIG. 3. (Color online) Temperature-dependence of susceptibility, charge fluctuations $\langle(\delta n)^2\rangle$, total spin S , and the spin-spin correlations $\langle S_1 \cdot S_2 \rangle$ of the 2-dot system.

plot combining the temperature dependence of the magnetic susceptibility and of other thermodynamic quantities, as presented in Fig. 3. Charge fluctuations $\langle(\delta n)^2\rangle$ show a sudden drop at $T \sim T_1^*$ representing the FO-LM transition. In contrast, the magnitude of the total spin S increases in steps: $S = 1/2, (\sqrt{7}-1)/2$, and 1. Values of S in these plateaus are the characteristic values of a doubly occupied double-quantum dot system in the FO, LM, and FF regimes, respectively.

The LM-FF transition temperature T_F^* can be deduced from the temperature dependence of the spin-spin correlation function. In the FF regime the spins tend to align, which leads to $\langle S_1 \cdot S_2 \rangle \rightarrow \sim 1/4$ as $T \rightarrow 0$, see Fig. 3. The transition from 0 to $1/4$ is realized at $T \sim T_F^*$. We can extract T_F^* using the (somewhat arbitrary) condition

$$\langle S_1 \cdot S_2 \rangle(T_F^*) = 1/2 \langle S_1 \cdot S_2 \rangle(T \rightarrow 0). \quad (32)$$

In Sec. VI B 1 we show that this condition is in very good agreement with $T_F^* = J_{\text{RKKY}}/\beta$ obtained by determining the explicit interimpurity antiferromagnetic coupling constant J_{12} , defined by the relation $J_{\text{RKKY}} + J_{12} = 0$ that destabilizes the high-spin $S = N/2$ state. The extracted T_F^* transition temperatures that correspond to plots in Fig. 2 are given in Table I. We find that they weakly depend on the number of impurities, more so than the Kondo temperature. The increase of T_F^* with N can be partially explained by calculating T_F^* for a spin Hamiltonian $H = -J_{\text{RKKY}} \sum_{i < j} \mathbf{S}_i \cdot \mathbf{S}_j$ for N spins decoupled from leads. Using Eq. (32) we obtain $T_F^* \approx 1.18 J_{\text{RKKY}}$ for $N=2$, $T_F^* \approx 1.36 J_{\text{RKKY}}$ for $N=3$, and $T_F^* \approx 1.55 J_{\text{RKKY}}$ for $N=4$.

By performing NRG calculations of T_F^* for other parameters U and Γ and comparing them to the prediction of the perturbation theory, we found that the simple formula (22) for J_{RKKY} agrees very well with numerical results.

The effect on thermodynamic properties of varying U while keeping Γ/U (i.e., $\rho_0 J_K$) fixed is illustrated in Fig. 4 for 2- and 3-dot systems. Parameters Γ and U enter expressions for $T_F^* = J_{\text{RKKY}}/\beta$ and T_K only through the ratio Γ/U , apart from the change of the effective bandwidth proportional to U , see Eqs. (5) and (22). This explains the horizon-

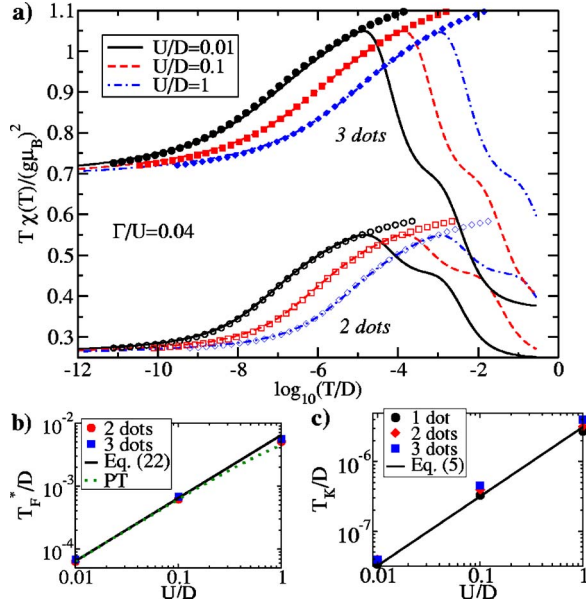


FIG. 4. (Color online) (a) Temperature-dependent susceptibility of the 2- and 3-dot systems with the same Γ/U ratio. Open (closed) symbols are Bethe ansatz results for the $S=1$ ($S=3/2$) Kondo model. (b) Comparison of LM-FF transition temperature T_F^* with predictions of the perturbation theory. (c) Comparison of calculated T_K with Haldane's formula.

tal shift towards higher temperatures of susceptibility curves with increasing U , as seen in Fig. 4(a). The NRG results and the Bethe Ansatz for the Kondo models with $S=1$ and $S=3/2$ show excellent agreement for $T < T_F^*$. In Figs. 4(b) and 4(c) we demonstrate the nearly linear U -dependence of T_F^* and T_K , respectively.

In Fig. 5 we show the effect of varying Γ/U while keeping U fixed. In this case, T_1^* stays the same, T_F^* is shifted quadratically, and T_K exponentially with increasing Γ/U . Figure 5(b) shows the agreement of T_F^* with expression (22), while Fig. 5(c) shows the agreement of the extracted values of T_K with formula (5).

We note that for $N \geq 2$, eventual coupling to an additional conduction channel (for example, due to a small asymmetry in the coupling to the source and drain electrodes) would lead to screening by additional half a unit of spin^{26,27} and the residual ground state spin would be $S-1=N/2-1$. For $N \geq 3$ and three channels (due to weak coupling to some third electrode), three half-units of spin would be screened, and so forth. These additional stages of Kondo screening would, however, occur at much lower temperatures; all our findings still apply at temperatures above subsequent Kondo crossovers.

In systems of multiple quantum dots, an additional screening mechanism is possible when after the first Kondo crossover, the residual interaction between the remaining spin and the Fermi liquid quasiparticles is anti-ferromagnetic.⁵⁰ This leads to an additional Kondo crossover at temperatures that are exponentially smaller than the first Kondo temperature. Such two-stage Kondo effect occurs, for example, in side-coupled double quantum dots⁵⁰⁻⁵³ and triple quantum dot coupled in series.⁵⁴ In parallelly coupled sys-

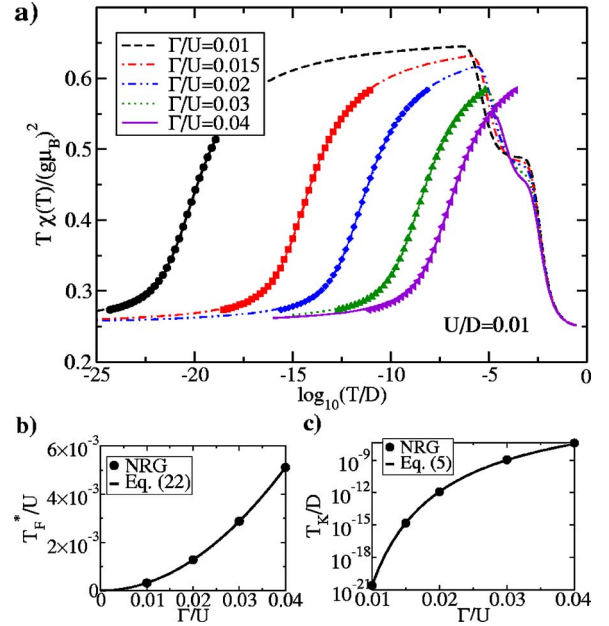


FIG. 5. (Color online) (a) Temperature-dependent susceptibility of the 2-dot system for equal $e-e$ repulsion $U/D=0.01$ and for different hybridization strengths Γ . Symbols represent the Bethe ansatz susceptibility for the $S=1$ Kondo model with corresponding T_K . (b) Comparison of calculated and predicted T_F^* . (c) Fit of T_K to Haldane's formula, Eq. (5).

tems, the residual interaction between the remaining spin and the Fermi liquid quasiparticles is, however, ferromagnetic as can be deduced from the splitting of the NRG energy levels in the strong-coupling fixed point:⁴⁹ the strong-coupling fixed point is stable.

We have thus demonstrated that with decreasing temperature the symmetric ($\delta=0$) multiple-impurity Anderson model flows from the FO regime, through LM and FF regimes, to a stable underscreened $S=N/2$ Kondo model strong-coupling fixed point. The summary of different regimes is given in Table II.

VI. STABILITY OF $N=2$ SYSTEMS WITH RESPECT TO VARIOUS PERTURBATIONS

We next explore the effect of various physically relevant perturbations with a special emphasis on the robustness of the ferromagnetically frozen state and the ensuing $S=N/2$ Kondo effect against perturbation of increasing strength. We show that the system of multiple quantum dots remains in a $S=N/2$ state even for relatively large perturbations. We also study the quantum phase transitions from the $S=N/2$ state driven by strong perturbations. In this section we limit our calculations to the $N=2$ system.

Unless otherwise noted, the parameters are still chosen well within the Kondo regime, $U/(\Gamma\pi) \gg 1$. We will show that the scale separation, as discussed in Sec. III, still holds for weak perturbations. It will also become evident that the quantum phase transitions are triggered precisely by the competition between various effects (such as magnetic order-

TABLE II. Regimes of the symmetric ($\delta=0$) N -impurity Anderson model.

Regime	Relevant states	Magnetic susceptibility $\mu_{\text{eff}}=T\chi_{\text{imp}}(T)/(g\mu_B)^2$	Spin correlations $\langle \mathbf{S}_1 \cdot \mathbf{S}_2 \rangle$	Charge fluctuations $\langle n^2 \rangle - \langle n \rangle^2$	Entropy S_{imp}
FO	$N \times (0\rangle, \uparrow\rangle, \downarrow\rangle, 2\rangle)$	$N/8$	0	$O(1)$	$N \ln 4$
LM	$N \times (\uparrow\rangle, \downarrow\rangle)$	$N/4$	0	small	$N \ln 2$
FF	$ S=N/2, S_z\rangle$	$N/2(N/2+1)/3$	$\sim 1/4$	small	$\ln(N+1)$
SC	$ S=N/2-1/2, S_z\rangle$	$(N-1)/2(N/2+1/2)/3$	$\sim 1/4$	small	$\ln N$

ing and Kondo screening) when any two energy scales become comparable.

A. Variation of the on-site energy levels

1. Deviation from the particle-hole symmetric point

A small departure from the particle-hole symmetric point ($\delta \neq 0$) does not destabilize the $S=N/2$ Kondo behavior: the magnetic susceptibility curves still follow the Bethe ansatz results even for δ/U as large as 0.4, see Fig. 6(a). For $\delta > \delta_c$, where $\delta_c/D \sim 0.45$ is the critical value of parameter δ , the triplet state is destabilized. Consequently, there is no Kondo effect. This is a particular case of the singlet-triplet transition that is a subject of intense studies in recent years, both experimentally^{55–57} and theoretically.^{36,53,58–60}

In the asymmetric single impurity model, the valence-fluctuation (VF) regime is characterized by $\mu_{\text{eff}} = T\chi(T)/(g\mu_B)^2 \sim 1/6$.³⁹ The VF regimes occur at T_1^* and the transition from the VF to LM regime occurs at $T_2^* \sim |E_d^*|/\alpha$,

where E_d^* is the renormalized on-site energy of the impurity: $E_d^* = \epsilon_d - \frac{1}{\pi} \ln(-U/E_d)$. For two uncorrelated dots in the VF regime, we expect $\mu_{\text{eff}} \sim 1/3$. In Fig. 6(a) we plotted a number of susceptibility curves for parameters δ in the proximity of the singlet-triplet transition. While there is no clearly observable valence-fluctuation plateau, the value of μ_{eff} is indeed near $1/3$ between T_1^* and $T_2^*(\delta_c)$.

In Fig. 6(b) we compare calculated Kondo temperatures with analytical predictions based on the results for the single impurity model.³⁹ For $\delta \neq 0$, J_K generalizes according to the Schrieffer-Wolff transformation, Eq. (15). Departure from the p-h symmetric point also induces potential scattering

$$\rho_0 K = \frac{\Gamma}{2\pi} \left(\frac{1}{|\delta - U/2|} - \frac{1}{|\delta + U/2|} \right). \quad (33)$$

The effective \tilde{J}_K that enters the expression for the Kondo temperature is³⁹

$$\tilde{J}_K = J_K [1 + (\pi \rho_0 K)^2], \quad (34)$$

and the effective bandwidth $0.182U$ is replaced by $0.182|E_d^*|$. The Kondo temperature is now given by

$$T_K = 0.182|E_d^*| \sqrt{\rho_0 \tilde{J}_K} \exp[-1/(\rho_0 \tilde{J}_K)]. \quad (35)$$

This analytical estimate agrees perfectly with the NRG results: for moderate δ/U , the results obtained for the asymmetric single impurity model also apply to the multiple-impurity Anderson model.

In Fig. 6(c) we show the δ -dependence of the LM-FF transition temperature T_F^* . Its value remains nearly independent of δ in the interval $\delta \leq 0.4U$ and then it suddenly drops. More quantitatively, the dependence on δ can be adequately described using an exponential function

$$T_F^*(\delta) = T_F^*(0) \left[1 - \exp\left(-\frac{\delta - \delta_c}{\lambda}\right) \right], \quad (36)$$

where $T_F^*(0)/D = 1.8 \times 10^{-5}$ is the transition temperature in the symmetric case, $\delta_c/D = 0.45$ is the critical δ , and $\lambda/D = 2.1 \times 10^{-2}$ is the width of the transition region. Exchange interaction J_{RKKY} does not depend on δ for $U/D = 0.01 \ll 1$, which explains the constant value of $T_F^*(\delta)$ for $\delta \leq 0.4U$. At a critical value δ_c , T_F^* goes to zero and for still higher δ the spin-spin correlation becomes antiferromagnetic. Since the ground-state spins are different, the triplet and singlet regimes are separated by a quantum phase transition at $\delta = \delta_c$. This transition is induced by charge fluctuations which destroy the ferromagnetic order of spins as the system enters

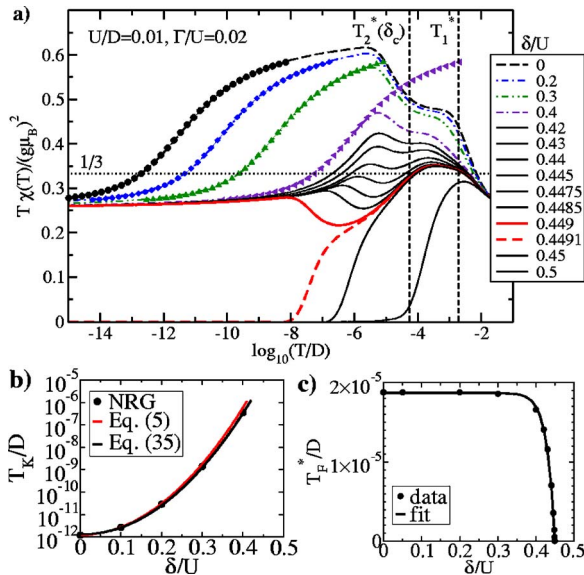


FIG. 6. (Color online) (a) Temperature-dependent susceptibility of the 2-dot systems on departure ($\delta > 0$) from the particle-hole symmetric point, $\delta=0$. Symbols are fits to the universal susceptibility obtained using the Bethe ansatz method for the $S=1$ Kondo model. (b) Calculated and predicted Kondo temperature, Eq. (35). For comparison we also plot T_K given by Eq. (5), which shows expected discrepancy for large δ/U . (c) Calculated T_F^* and the fit to an exponential function.

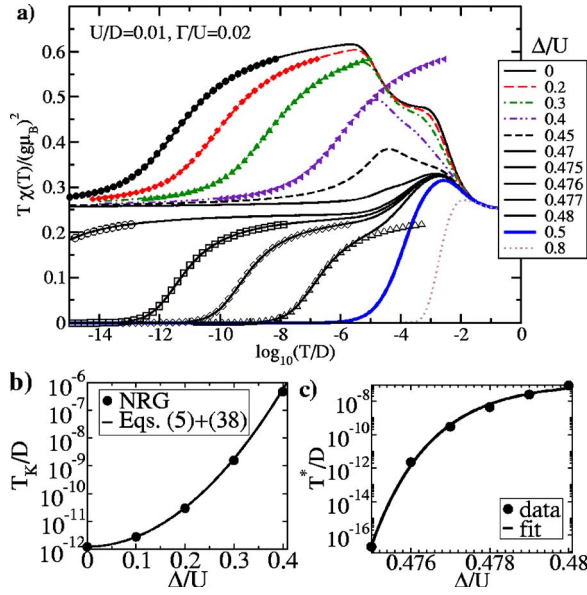


FIG. 7. (Color online) (a) Temperature-dependent susceptibility of the 2-dot system with unequal (detuned) on-site energies, $\delta_1 = \Delta$, $\delta_2 = -\Delta$. Full symbols present Bethe ansatz results of the equivalent $S=1$ Kondo model, while empty symbols are BA results of a $S=1/2$ Kondo model. (b) Comparison of calculated and predicted Kondo temperature, see Eqs. (5) and (38). (c) The Kondo temperature of the $S=1/2$ Kondo screening on the singlet side of the transition and a fit to Eq. (39).

the VF regime. The exponential dependence arises from the grand-canonical statistical weight factor $\exp[\delta(n-2)/(k_B T)]$, where n is the number of the electrons confined on the dots. The transition is of the first order, since for equal coupling of both impurities to the band there is no mixing between the $n=2$ triplet states and the $n=0$ singlet state.⁵⁰

For δ slightly lower than the critical δ_c , the effective moment $T\chi(T)$ shows a rather unusual temperature dependence. It first starts decreasing due to charge fluctuations, however, with further lowering of the temperature the moment ordering wins over, $T\chi(T)$ increases, and at low-temperatures approaches the value characteristic for the partially screened $S=1$ moment, i.e., $T\chi/(g\mu_B)^2 \sim 1/4$.

2. Splitting of the on-site energy levels

We next consider the 2-dot Hamiltonian with unequal on-site energies δ_i :

$$H_{\text{dot},i} = \delta_i(n_i - 1) + \frac{U}{2}(n_i - 1)^2. \quad (37)$$

We focus on the case $\delta_1 = \Delta$ and $\delta_2 = -\Delta$, which represents another experimentally relevant perturbation. This model is namely particle-hole symmetric for an arbitrary choice of Δ under a generalized p-h transformation $c_{k\sigma}^\dagger \rightarrow c_{k,-\sigma}$, $d_{1\sigma}^\dagger \rightarrow d_{2,-\sigma}$, $d_{2\sigma}^\dagger \rightarrow d_{1,-\sigma}$. The total occupancy of both dots is exactly 2 for any Δ . We can therefore study the effect of the on-site energy splitting while maintaining the particle-hole symmetry. Susceptibility curves are shown in Fig. 7(a) for a range of values of Δ . For Δ up to some critical value

$\Delta_c \approx 0.47$ the 2-dot Anderson model remains equivalent to the $S=1$ Kondo model for $T < T_F^*$. A singlet-triplet transition of the Kosterlitz-Thouless type^{50,53} occurs at $\Delta = \Delta_c$.

Even though the two dots are now inequivalent, the Schrieffer-Wolff transformation yields the same J_K for both spin impurities. We obtain

$$J_K = 2|V_{k_F}|^2 \left(\frac{1}{|\Delta - U/2|} + \frac{1}{|\Delta + U/2|} \right). \quad (38)$$

Due to the particle-hole symmetry no potential scattering is generated. The effective Kondo Hamiltonian for small Δ is thus nearly the same as that for small δ discussed in the previous section. In Fig. 7(b) calculated Kondo temperatures are plotted in comparison with analytical result from Eqs. (5) and (38). The agreement is excellent.

The properties of the systems with $\delta \neq 0$ and $\Delta \neq 0$ become markedly different near respective singlet-triplet transition points. For $\delta \neq 0$, the transition is induced by charge fluctuations which suppress magnetic ordering and, due to equal coupling of both dots to the band, the transition is of first order. For $\Delta \neq 0$ the transition is induced by depopulating dot 2 and populating dot 1 while the total charge on the dots is maintained, which leads to the transition from an interimpurity triplet to a local spin-singlet on the dot 1. Since there is an asymmetry between the dots, the transition is of the Kosterlitz-Thouless type.⁵⁰

The Kondo temperature of the $S=1/2$ Kondo screening near the transition on the singlet side, T^* , is approximately given by

$$\log T^*/D = -\alpha - \beta \exp\left(-\frac{\Delta - \tilde{\Delta}}{\lambda}\right). \quad (39)$$

We obtain $\alpha \approx 7$, $\beta \approx 2.8$, $\tilde{\Delta}/D \approx 0.477$, and $\lambda/D \approx 1.5 \times 10^{-3}$. This expression is consistent with the crossover scale formula $T^* \propto \exp[-T_K/J_{12}]$ for a system of two fictitious spins, one directly coupled to the conduction band and the other side-coupled to the first one with exchange-interaction J_{12} that depends exponentially on Δ : $J_{12} = T_K/\beta \exp[(\Delta - \tilde{\Delta})/\lambda]$.

B. Interimpurity interaction

1. Interimpurity exchange interaction

In this section we show that by introducing an explicit exchange interaction J_{12} between the localized spins on the dots, the strength of the RKKY interaction, J_{RKKY} , can be directly determined. We thus study the two-impurity Anderson model with

$$H_{\text{dots}} = \sum_{i=1}^2 H_{\text{dot},i} + J_{12} \mathbf{S}_1 \cdot \mathbf{S}_2,$$

where $J_{12} > 0$.

As seen from Fig. 8, for J_{12} above a critical value J_c , the RKKY interaction is compensated, local moments on the dots form the singlet rather than the triplet which in turn prevents formation of the $S=1$ Kondo effect. The phase tran-

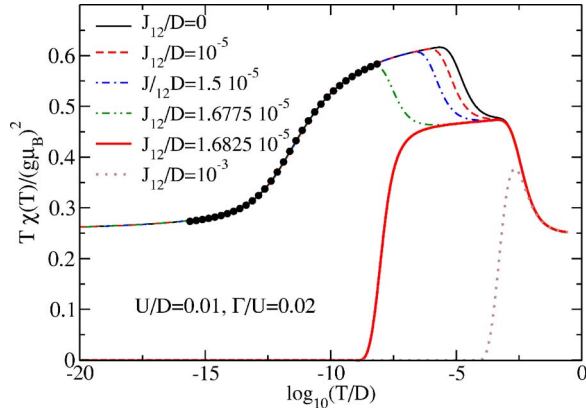


FIG. 8. (Color online) Temperature-dependent susceptibility of the 2-dot systems for different antiferromagnetic interimpurity couplings J_{12} . Circles are Bethe ansatz results for the susceptibility of the $S=1$ Kondo model with the Kondo temperature which is equal for all cases where $J_{12} < J_c$.

sition is of the first order.⁵⁰ Using Eq. (32), we obtain $T_F^*/D \approx 1.87 \times 10^{-5}$ for the nonperturbed problem with the same U and Γ , while $J_c/D \approx 1.68 \times 10^{-5}$. Taking into account the definition $T_F^* = J_{\text{RKKY}}/\beta$, where $\beta \sim 1$, we conclude that J_{RKKY} agrees well with the critical value of J_c , i.e., $J_c = J_{\text{RKKY}}$. The perturbation theory prediction of $J_{\text{RKKY}}/D = 1.6 \times 10^{-5}$ also agrees favorably with numerical results.

As long as $J_{12} < J_c$, even for $J_{12} > T_K$, the $S=1$ Kondo effect survives and, moreover, the Kondo temperature remains unchanged, determined only by the value of $\rho_0 J_K$ as in the $J_{12}=0$ case. The only effect of increasing J_{12} in the regime where $J_{12} < J_c$ is the reduction of the transition temperature into the triplet state, which is now given by $T_F \sim J_{\text{eff}}/\beta$ with the effective interimpurity interaction $J_{\text{eff}} = J_{\text{RKKY}} - J_{12}$.

2. Hopping between the impurities

We now study the two-impurity Anderson model with additional hopping between the dots:

$$H_{\text{dots}} = \sum_{i=1}^2 H_{\text{dot},i} - t_{12} \sum_{\sigma} (d_{1\sigma}^\dagger d_{2\sigma} + d_{2\sigma}^\dagger d_{1\sigma}). \quad (40)$$

This model can be viewed also as a single-channel version of the Alexander-Anderson model⁶¹ in the limit of zero separation between the impurities. The magnetic-susceptibility curves are shown in Fig. 9.

The hopping leads to hybridization between the atomic levels of the dots which in turn results in the formation of an even and odd level (“molecular orbital”) with energies $\epsilon_{e,o} = \epsilon_d \pm t_{12}$. In the presence of interaction U there are two contributions to the energy of the low-lying states: “orbital energy” proportional to t_{12} and “magnetic energy” due to an effective antiferromagnetic exchange $J_{\text{AFM}} = 4t_{12}^2/U$, which is second order in t_{12} . Even though the orbital energy is the larger energy scale, the Kondo effect is largely insensitive to the resulting level splitting. Instead, the Kondo effect is destroyed when J_{AFM} exceeds J_{RKKY} , much like in the case of explicit exchange interaction between the dots which was

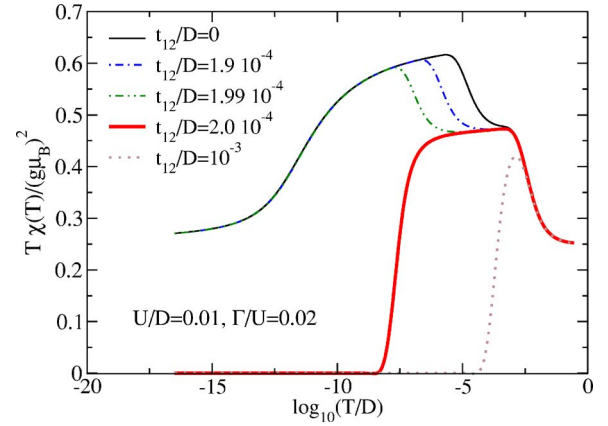


FIG. 9. (Color online) Temperature-dependent susceptibility of the 2-dot systems with interdot tunneling coupling t_{12} . For $t_{12}/D \approx 2 \times 10^{-4}$, we have $J_{\text{AFM}}/D \approx 1.6 \times 10^{-5}$, which agrees well with the critical value of $J_c/D \approx 1.7 \times 10^{-5}$ found in the case of an explicit exchange interaction between the dots, see Fig. 8.

discussed in the previous section. We should emphasize the similarity between the curves in Figs. 8 and 9.

In the wideband limit $U \ll D$, $J_{\text{RKKY}}/D \approx 0.62 \times 64/\pi^2 \Gamma^2/U$, therefore the critical $t_{12,c}$ is given by $t_{12,c} \approx \Gamma$ and it does not depend on U . This provides an alternative interpretation for the U -dependence of $t_{12,c}$ in the strong-coupling regime found in Ref. 62.

C. Isospin-invariance breaking perturbations

The interimpurity electron repulsion and the two-electron hopping between the impurities represent perturbations that break the isospin $SU(2)$ symmetry of the original model, while they preserve both the particle-hole symmetry as well as the spin invariance.

1. Interimpurity electron repulsion

The effect of the interimpurity electron repulsion (induced by capacitive coupling between the two parallel quantum dots) is studied using the Hamiltonian

$$H_{\text{dots}} = \sum_{i=1}^2 H_{\text{dot},i} + U_{12}(n_1 - 1)(n_2 - 1), \quad (41)$$

where it should be noted that $(n_1 - 1)(n_2 - 1) = 4I_1^z I_2^z$ is the longitudinal part of the isospin-isospin exchange interaction $\mathbf{I}_1 \cdot \mathbf{I}_2$. This perturbation breaks the $SU(2)_{\text{iso}}$ symmetry to $U(1)_{\text{gauge}} \times Z_2$ symmetry, where $U(1)_{\text{gauge}}$ corresponds to rotations around the isospin z -axis (I_z , i.e., charge, is still a good quantum number) and Z_2 corresponds to permutations of isospin x and y axis.

Results in Fig. 10 show that the interimpurity repulsion is not an important perturbation as long as $U_{12} < U$. Finite U_{12} only modifies the Kondo temperature and the temperature T_1^* of the FO-LM transition, while the behavior of the system remains qualitatively unchanged. Note that T_F^* is unchanged since U_{12} equally affects both the singlet and the triplet energy.

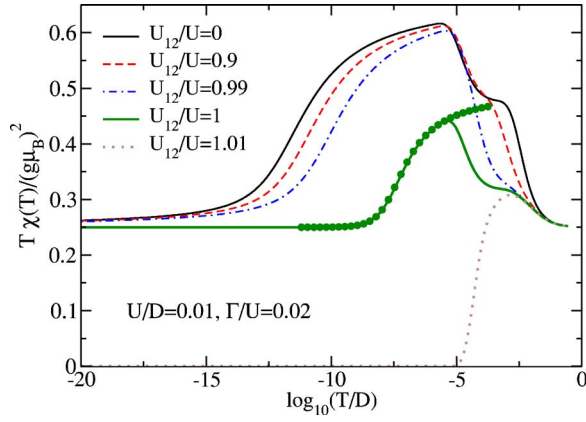


FIG. 10. (Color online) Temperature-dependent susceptibility of the 2-dot systems for different interimpurity electron-electron repulsion parameters U_{12} . Circles are the Bethe ansatz results for the $S = 1/2$ Kondo model which fit the NRG results in the special case $U_{12}=U$.

For $U_{12} > U$ the electrons can lower their energy by forming on-site singlets and the system enters the *charge-ordering regime*.⁶³ This behavior bares some resemblance to that of the negative- U Anderson model⁶⁴ which undergoes a charge Kondo effect.

The system behaves in a peculiar way at the transition point $U_{12}=U$ where U_{12} and U terms can be combined using isospin operators as

$$U/2[4(I_1^z)^2 + 4(I_2^z)^2] + U_{12}4I_1^z I_2^z = 2U(I^z)^2. \quad (42)$$

We now have an intermediate temperature fixed point with a sixfold symmetry of states with $I_z=0$ as can be deduced from Eq. (42) and the entropy curve in Fig. 11.

While the $SU(2)_{\text{iso}}$ isospin symmetry is broken for any $U_{12} \neq 0$ to $U(1)_{\text{gauge}} \times Z_2$, a new orbital $SU(2)_{\text{orb}}$ pseudospin (approximate) symmetry appears at the special point $U_{12}=U$. For two impurities we can define an orbital pseudospin operator as

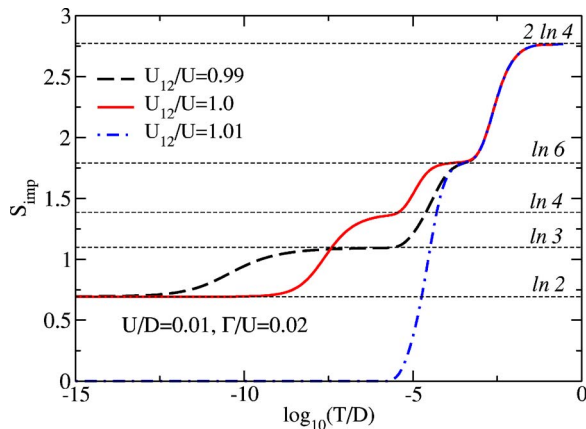


FIG. 11. (Color online) Temperature-dependent entropy of the 2-dot systems for different interimpurity electron-electron repulsion U_{12} .

$$\mathbf{O} = \frac{1}{2} \sum_{\alpha} \sum_{i,j=1,2} d_{i\alpha}^{\dagger} \boldsymbol{\sigma}_{ij} d_{j\alpha}, \quad (43)$$

where $\boldsymbol{\sigma}$ is the vector of the Pauli matrices. Note that the orbital pseudospin and isospin operators do not all commute, therefore the full orbital pseudospin and isospin $SU(2)$ symmetries are mutually exclusive. The quantum dots Hamiltonian H_{dots} commutes for $U_{12}=U$ with all three components of the orbital pseudospin operator; the decoupled impurities thus have orbital $SU(2)_{\text{orb}}$ symmetry. Furthermore, pseudospin \mathbf{O} and spin \mathbf{S} operators commute and the symmetry is larger, $SU(2)_{\text{spin}} \otimes SU(2)_{\text{orb}}$. In fact, the set of three S^i , three O^i , and nine operators $S^i O^j$ are the generators of the $SU(4)$ symmetry group of which $SU(2)_{\text{spin}} \otimes SU(2)_{\text{orb}}$ is a subgroup. The six degenerate states are the spin triplet, orbital singlet and the spin singlet, orbital triplet⁶⁵ which form a $SU(4)$ sextet:

$$|S=1, S_z=1, O=0\rangle = |\uparrow, \uparrow\rangle,$$

$$|S=1, S_z=0, O=0\rangle = 1/\sqrt{2}(|\uparrow, \downarrow\rangle + |\downarrow, \uparrow\rangle),$$

$$|S=1, S_z=-1, O=0\rangle = |\downarrow, \downarrow\rangle,$$

$$|S=0, O=1, O_z=1\rangle = |\uparrow\downarrow, 0\rangle,$$

$$|S=0, O=1, O_z=0\rangle = 1/\sqrt{2}(|\uparrow, \downarrow\rangle - |\downarrow, \uparrow\rangle),$$

$$|S=0, O=1, O_z=-1\rangle = |0, \uparrow\downarrow\rangle.$$

It should be noted that the orbital pseudospin eigenstates $|S=0, O=1, O_z=\pm 1\rangle$ can be combined into an isospin triplet eigenstate $|S=0, I=1, I_z=0\rangle = 1/\sqrt{2}(|\uparrow\downarrow, 0\rangle + |0, \uparrow\downarrow\rangle)$ and an isospin singlet eigenstate $|S=0, I=0\rangle = 1/\sqrt{2}(|\uparrow\downarrow, 0\rangle - |0, \uparrow\downarrow\rangle)$. This recombination is possible because I_z [$U(1)_{\text{gauge}}$ charge operator] commutes with both the Hamiltonian [see Eq. (42)] and the orbital pseudospin operators.

The coupling of impurities to the leads, however, breaks the orbital symmetry. Unlike the model studied in Ref. 63, our total Hamiltonian H is not explicitly $SU(4)$ symmetric, and unlike in the model studied in Ref. 66, in our system this symmetry is not dynamically (re)established on the scale of the Kondo temperature. No $SU(4)$ Kondo effect is therefore expected. Instead, as the temperature decreases the degeneracy first drops from 6 to 4 and then from 4 to 2 in a $S = 1/2$ $SU(2)$ Kondo effect (see the fit to the Bethe ansatz result in Fig. 10). There is a residual twofold degeneracy in the ground state. To understand these results, we applied perturbation theory (Appendix A) which shows that the sextuplet splits in the fourth order perturbation in V_k . The spin-triplet states and the state $|S=0, I=0\rangle$ form the new fourfold degenerate low-energy subset of states, while the states $|S=0, I=1, I_z=0\rangle$ and $|S=0, O=1, O_z=0\rangle$ have higher energy. The remaining four states can be expressed in terms of even and odd molecular-orbitals described by operators $d_{e\sigma}^{\dagger} = 1/\sqrt{2}(d_{1\sigma}^{\dagger} + d_{2\sigma}^{\dagger})$ and $d_{o\sigma}^{\dagger} = 1/\sqrt{2}(d_{1\sigma}^{\dagger} - d_{2\sigma}^{\dagger})$. We obtain

$$|S=1, S_z=1, O=0\rangle = d_{e,\uparrow}^{\dagger} d_{o,\uparrow}^{\dagger} |0\rangle,$$

$$\begin{aligned}
 |S = 1, S_z = 0, O = 0\rangle &= 1/\sqrt{2}(d_{o,\uparrow}^\dagger d_{e,\downarrow}^\dagger + d_{e,\uparrow}^\dagger d_{o,\downarrow}^\dagger)|0\rangle, \\
 |S = 1, S_z = -1, O = 0\rangle &= d_{e,\downarrow}^\dagger d_{o,\downarrow}^\dagger|0\rangle, \\
 |S = 0, I = 0\rangle &= 1/\sqrt{2}(d_{o,\uparrow}^\dagger d_{e,\downarrow}^\dagger - d_{e,\uparrow}^\dagger d_{o,\downarrow}^\dagger)|0\rangle. \quad (44)
 \end{aligned}$$

The four remaining states are therefore a product of a spin-doublet in the even orbital and a spin-doublet in the odd orbital. Due to the symmetry of our problem, only the even orbital couples to the leads, while the odd orbital is entirely decoupled. The electron in the even orbital undergoes $S = 1/2$ Kondo screening, while the unscreened electron in the odd orbital is responsible for the residual twofold degeneracy.

2. Two-electron hopping

We consider the Hamiltonian

$$H_{\text{dots}} = \sum_{i=1}^2 H_{\text{dot},i} - T_{12} \hat{T}, \quad (45)$$

where \hat{T} is the two-electron hopping operator that can be expressed in terms of the transverse part of the isospin-isospin exchange interaction $\mathbf{I}_1 \cdot \mathbf{I}_2$:

$$\hat{T} = d_{1\uparrow}^\dagger d_{1\downarrow}^\dagger d_{2\downarrow} d_{2\uparrow} + d_{2\uparrow}^\dagger d_{2\downarrow}^\dagger d_{1\downarrow} d_{1\uparrow} = I_1^+ I_2^- + I_1^- I_2^+ = 2(I_1^x I_2^x + I_1^y I_2^y). \quad (46)$$

This perturbation term is complementary to the one generated by U_{12} in Eq. (42) and studied in the previous section. Physically, it corresponds to correlated tunneling of electron pairs which can be neglected in the applications to problems of transport through parallel quantum dots coupled electrostatically as physically realized in semiconductor heterostructures. Models featuring pair-tunneling terms as in Eq. (46) may, however, be of interest to problems in tunneling through molecules with vibrational degrees of freedom, where ground states with an even number of electrons can be favored due to a polaronic energy shift.^{67,68} In such cases, the charge transport is expected to be dominated by the electron-pair tunneling.⁶⁸

The temperature dependence of the magnetic susceptibility shown in Fig. 12 again demonstrates the robustness of the $S=1$ state for $|T_{12}| < U$. The behavior of the system for negative T_{12} is similar to the case of the interimpurity repulsion. For $T_{12} = -U$ we again observe special behavior of the susceptibility curve, characteristic for the sixfold degeneracy observed in the previous section at $U_{12} = U$. For positive T_{12} the system undergoes the $S=1$ spin Kondo effect up to and including $T_{12} = U$. The FO-LM transition temperature T_1^* and the Kondo temperature are largely T_{12} independent, while the LM-FF transition temperature T_F^* decreases with increasing T_{12} .

D. Unequal coupling to the continuum

We finally study the Hamiltonian that allows for unequal hybridizations $\Gamma_i = \pi\rho_0 |V_{k_i}^i|^2$ in the following form:

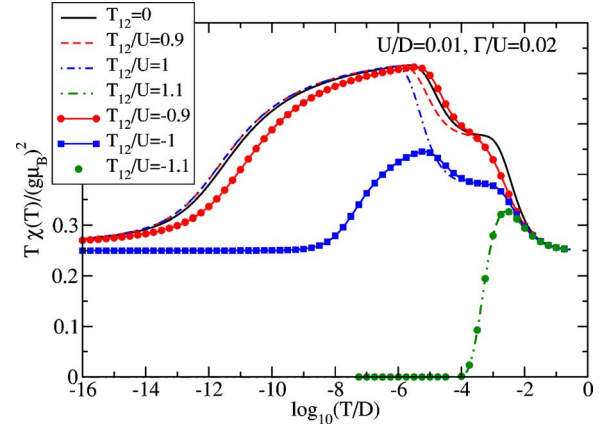


FIG. 12. (Color online) Temperature-dependent susceptibility of the 2-dot system with two-electron hopping between the dots T_{12} .

$$H = H_{\text{band}} + H_{\text{dots}} + \sum_{i=1}^2 H_{c,i}, \quad (47)$$

with

$$H_{c,i} = \frac{1}{\sqrt{L}} \sum_{k\sigma} (V_k^i d_{i\sigma}^\dagger c_{k\sigma} + \text{H.c.}). \quad (48)$$

We set $V_k^2 = \alpha V_k^1$, i.e., $\Gamma_2 = \alpha^2 \Gamma_1$.

The effective low-temperature Hamiltonian can be now written as

$$H_{\text{eff}} = H_{\text{band}} + s \cdot \sum_{i=1}^2 J_{K,i} \mathbf{S}_i - J_{\text{RKKY}}^{\text{eff}} \mathbf{S}_1 \cdot \mathbf{S}_2, \quad (49)$$

with $J_{K,2} = \alpha^2 J_{K,1}$ and with the effective RKKY exchange interaction given by a generalization of Eq. (21)

$$J_{\text{RKKY}}^{\text{eff}} = 0.62 U \rho_0^2 J_{K,1} J_{K,2} = \alpha^2 J_{\text{RKKY}}, \quad (50)$$

where J_{RKKY} is the value of the RKKY parameter at $\alpha = 1$. In our attempt to derive the effective Hamiltonian we assume that in the temperature regime $T \lesssim J_{\text{RKKY}}^{\text{eff}}$ the two moments couple into a triplet. Since the two Kondo exchange constants $J_{K,i}$ are now different, we rewrite H_{eff} in Eq. (49) in the following form:

$$\begin{aligned}
 H_{\text{eff}} = H_{\text{band}} + s \cdot & \left(\frac{J_{K,1} + J_{K,2}}{2} (\mathbf{S}_1 + \mathbf{S}_2) \right) \\
 + s \cdot & \left(\frac{J_{K,1} - J_{K,2}}{2} (\mathbf{S}_1 - \mathbf{S}_2) \right) - J_{\text{RKKY}}^{\text{eff}} \mathbf{S}_1 \cdot \mathbf{S}_2. \quad (51)
 \end{aligned}$$

Within the triplet subspace, $\mathbf{S}_1 + \mathbf{S}_2$ is equal to the new composite spin 1, which we denote by \mathbf{S} , $\mathbf{S}_1 - \mathbf{S}_2$ is identically equal to zero, and $\mathbf{S}_1 \cdot \mathbf{S}_2$ is a constant $-1/4$. As a result, the effective J_K is simply the average of the two exchange constants:

$$J_{K,\text{eff}} = \frac{J_{K,1} + J_{K,2}}{2}. \quad (52)$$

Susceptibility curves for different α are shown in Fig. 13. Note that the Kondo temperature determined using Eq. (5)

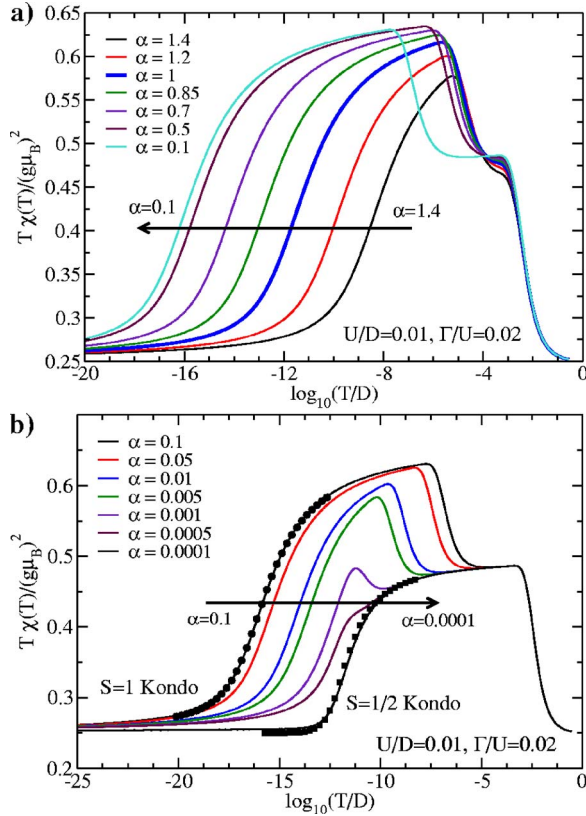


FIG. 13. (Color online) Temperature-dependent susceptibility of the 2-dot system with unequal coupling to the leads, $\Gamma_2 = \alpha^2 \Gamma_1$. (a) The range of α where T_K is decreasing. (b) The range of α where T_K is increasing again. Circles (squares) are BA results for the $S = 1$ ($S = 1/2$) Kondo model. The arrows indicate the evolution of the susceptibility curves as the parameter α decreases.

combined with the naive argument given in Eq. (52) fails to describe the actual Kondo scale for $\alpha \lesssim 0.4$ as seen from Fig. 14. This is due to admixture of the singlet state, which also renormalizes J_K , even though the singlet is separated by $J_{\text{RKKY}}^{\text{eff}} \gg T_K$ from the triplet subspace. Note, however, that $J_{\text{RKKY}}^{\text{eff}}$ is well-described by the simple expression given in Eq. (50) as shown in Fig. 14. By performing a second-order RG calculation (see Appendix B), which takes the admixture of the singlet state into account, we obtain T_K as a function of α which agrees very well with the NRG results, see Fig. 14.

For extremely small α , $J_{\text{RKKY}}^{\text{eff}}$ eventually becomes comparable to the Kondo temperature, see Fig. 14. For that reason the ferromagnetic locking-in is destroyed and the system behaves as a double $S = 1/2$ doublet, one of which is screened at $T_K^1 = T_K(J_{K,1})$ as shown in Fig. 13(b).

VII. CONCLUSIONS

We have shown that several magnetic impurities, coupled to the same Wannier orbital of a conduction electron band, experience ferromagnetic RKKY interaction which locks

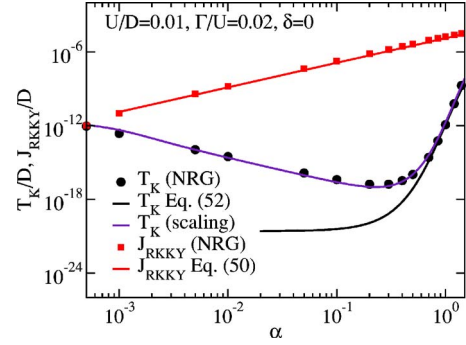


FIG. 14. (Color online) Comparison of calculated and predicted Kondo temperature T_K and effective exchange interaction $J_{\text{RKKY}}^{\text{eff}}$. The calculation of scaling results for T_K is described in Appendix B.

local moments in a state of a maximal total spin. The multiple-impurity Anderson model is at low temperatures, i.e., for $T < T_F^*$, equivalent to a $S = N/2$ $SU(2)$ Kondo model. Using perturbation theory up to the fourth order in V we derived an analytical expression for J_{RKKY} and tested it against NRG calculations. We have also shown that the high-spin state is very robust against experimentally relevant perturbations such as particle-hole symmetry breaking, on-site energy level splitting, interimpurity capacitive coupling, and direct exchange interaction. At low temperatures, the ferromagnetically locked impurities undergo a collective Kondo crossover in which half of a unit of spin is screened. The Kondo temperature in this simple model does not depend on the total spin (i.e., on the number of impurities N), while the LM-FF temperature T_F^* is weakly N -dependent.

We next list a few of the most important findings concerning the effect of various perturbations to the original two-dot system. (a) T_F^* is in the range $\delta \lesssim 0.4U$ nearly independent of the deviation from the particle-hole symmetric point $\delta = 0$. (b) Increasing the difference between on-site energies of two dots, 2Δ , induces a Kosterlitz-Thouless type phase transition separating the phase with $S = 1/2$ residual spin at low temperatures from the $S = 0$ one. (c) Introduction of additional one-electron hopping between the impurities induces effective AFM interaction $J_{\text{AFM}} = 4t_{12}^2/U$ that does not affect the Kondo temperature as long as $J_{\text{AFM}} \lesssim J_{\text{RKKY}}$, nevertheless, at $t_{12} = t_{12,c}$ it destabilizes the $S = 1$ state. The critical value $t_{12,c} \sim \Gamma$ does not depend on U . (d) Interimpurity Coulomb interaction U_{12} leads to a transition from the $S = 1$ Kondo state to the charge ordered state. In the four-fold degenerate intermediate point, reached at $U_{12} = U$, the effective Hamiltonian consists of the effective $S = 1/2$ Kondo model and of a free, decoupled $S = 1/2$ spin. (e) When the two impurities are coupled to the leads with different hybridization strengths, second-order scaling equations provide a good description of the Kondo temperature.

The properties of our model apply very generally, since high-spin states can arise whenever the RKKY interaction is ferromagnetic, even when the dots are separated in space.^{34,69} In addition, it has become possible to study Kondo physics in clusters of magnetic atoms on metallic surfaces.^{8,70} On (111) facets of noble metals such as copper, bulk electrons coexist with Shockley surface-state electrons.⁷¹ Surface-state bands on these surfaces have

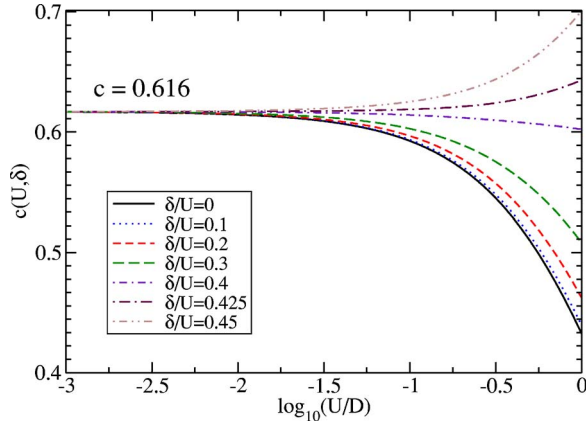


FIG. 15. (Color online) The prefactor c in the RKKY exchange constant $J_{\text{RKKY}} = c16V^4/(D^2U)$ for a flatband with $\rho_0 = 1/(2D)$ as a function of U for a range of values of the impurity energy level δ .

$k_F \sim 0.1 - 0.2 \text{ \AA}^{-1}$; thus for nearest and next-nearest neighbor adatoms $k_F R \lesssim 1$. If hybridization to the surface band is dominant, small clusters then effectively couple to the same Wannier orbital of the surface band and the single-channel multiple-impurity Anderson model is applicable; in the absence of additional interimpurity interactions, the spins would then tend to order ferromagnetically. If hybridization to the bulk band with $k_F^{\text{3D}} \sim 1 \text{ \AA}^{-1}$ is also important, the problem must be described using a complex two-band multichannel Hamiltonian.

Another relevant application of multiple-impurity models is to magnetic atoms confined to quantum corrals. Calculations of interimpurity interaction between two magnetic atoms located at the foci of an elliptical quantum corral indicate that the quantum corral eigenmode mediated exchange interaction is ferromagnetic.^{72,73}

Further aspects of the multiple-impurity Anderson model should be addressed in future work. Systems of coupled quantum dots and magnetic impurities on surfaces are mainly characterized by measuring their transport properties. Conductance can be determined by calculating the spectral density functions using the numerical renormalization group method. We anticipate that the fully screened $N=1$ model will have different temperature dependence as the under-screened $N \geq 2$ models. Since in quantum dots the impurity level δ (or ϵ_d) can be controlled using gate voltages, it should be interesting to extend the study to asymmetric multiple-impurity models for $N > 2$ where more quantum phase transitions are expected in addition to the one already identified for $N=2$ at $\delta = \delta_c$.

ACKNOWLEDGMENTS

The authors acknowledge useful discussions with J. Mravlje and L. G. Dias da Silva and the financial support of the SRA under Grant No. P1-0044.

APPENDIX A: RAYLEIGH-SCHROEDINGER PERTURBATION THEORY IN V_k

Following Ref. 74, we apply Rayleigh-Schrödinger perturbation theory to calculate second and fourth order corrections in V_k to the energy of a state $|n\rangle$:

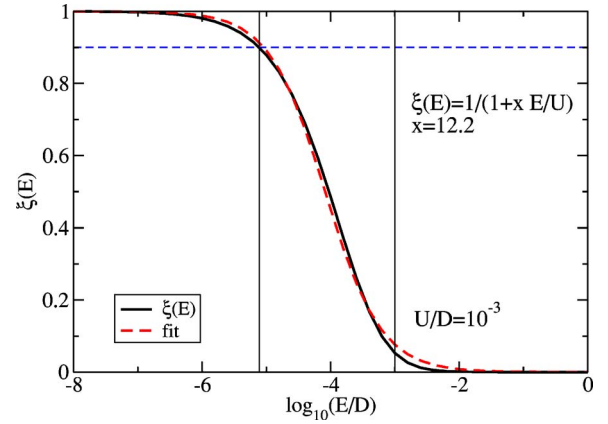


FIG. 16. (Color online) Ratio $\xi(E) = J_{\text{RKKY}}(E)/J_{\text{RKKY}}^0$ of the running RKKY coupling constant at energy E over its value in the $E \rightarrow 0$ limit. The dashed line is an approximate fit to a simple rational function $\xi(E) = 1/(1+xE/U)$.

$$E_n^{(2)} = \sum'_m \frac{\langle n|H_c|m\rangle\langle m|H_c|n\rangle}{E_n - E_m},$$

$$E_n^{(4)} = \sum'_{m_1, m_2, m_3} \frac{\langle n|H_c|m_3\rangle\langle m_3|H_c|m_2\rangle\langle m_2|H_c|m_1\rangle\langle m_1|H_c|n\rangle}{(E_n - E_{m_3})(E_n - E_{m_2})(E_n - E_{m_1})}. \quad (\text{A1})$$

The summation extends over all intermediate states $|m_i\rangle$ not equal to one of the degenerate ground states. We will consider the simplified case of constant V_k , i.e., $V_k = V_{k_F} = V$.

1. RKKY interaction in the two-impurity case

We study the splitting between the singlet $|S\rangle = 1/\sqrt{2}(|\uparrow, \downarrow\rangle - |\downarrow, \uparrow\rangle)$ and the triplet state $|T\rangle = 1/\sqrt{2}(|\uparrow, \downarrow\rangle + |\downarrow, \uparrow\rangle)$. The second order corrections are $E_S^{(2)} = E_T^{(2)} = -(S_1 + S_2)$ with

$$S_1 = 4V^2 \frac{1}{L} \sum_{k' \geq k_F} \frac{1}{U - 2\delta + 2\epsilon_{k'}},$$

$$S_2 = 4V^2 \frac{1}{L} \sum_{k \leq k_F} \frac{1}{U + 2\delta - 2\epsilon_k}. \quad (\text{A2})$$

There is therefore no splitting to this order in V . The fourth order corrections are

$$E_S^{(4)} = W_S^{\text{ph}} + W_S^{\text{pp}} + W_S^{\text{hh}},$$

$$E_T^{(4)} = W_T^{\text{ph}}, \quad (\text{A3})$$

where the particle-hole (ph), particle-particle (pp), and hole-hole (hh) intermediate-state contributions are

$$\begin{aligned}
W_S^{\text{ph}} &= \frac{16V^4}{U} \frac{1}{L^2} \sum_{k \leq k_F, k' > k_F} \frac{8(\delta - \epsilon_k)(\delta - \epsilon_{k'})(U + \epsilon_k - \epsilon_{k'})}{(U - 2\delta + 2\epsilon_k)^2 (U + 2\delta - 2\epsilon_{k'})^2 (\epsilon_k - \epsilon_{k'})}, \\
W_T^{\text{ph}} &= 32V^4 \frac{1}{L^2} \sum_{k \leq k_F, k' > k_F} \frac{2U^2 + 5U(\epsilon_k - \epsilon_{k'}) + 4[\delta^2 + \epsilon_k^2 + \epsilon_{k'}^2 - \epsilon_k \epsilon_{k'} - \delta(\epsilon_k + \epsilon_{k'})]}{(U - 2\delta + 2\epsilon_k)^2 (U + 2\delta - 2\epsilon_{k'})^2 (\epsilon_k - \epsilon_{k'})}, \\
W_S^{\text{pp}} &= \frac{16V^4}{U} \frac{1}{L^2} \sum_{k_1' > k_F, k_2' > k_F} \frac{2(U - 2\delta)(3U - 2\delta) + 8(U - \delta)(\epsilon_{k_1'} + \epsilon_{k_2'}) + 8\epsilon_{k_1'} \epsilon_{k_2'}}{(U - 2\delta + 2\epsilon_{k_1'})^2 (U - 2\delta + 2\epsilon_{k_2'})^2}, \\
W_S^{\text{hh}} &= \frac{16V^4}{U} \frac{1}{L^2} \sum_{k_1 \leq k_F, k_2 \leq k_F} \frac{2(U + 2\delta)(3U + 2\delta) - 8(U + \delta)(\epsilon_{k_1} + \epsilon_{k_2}) + 8\epsilon_{k_1} \epsilon_{k_2}}{(U + 2\delta - 2\epsilon_{k_1})^2 (U + 2\delta - 2\epsilon_{k_2})^2}.
\end{aligned} \tag{A4}$$

From these expressions we obtain $J_{\text{RKKY}} = E_S - E_T$. In order to evaluate the sums for a flatband with a constant density of states $\rho_0 = 1/(2D)$ and the chemical potential $\mu = 0$, we make formal replacements $\frac{1}{L} \sum_{k' > k_F} = \frac{1}{L} \sum_{k' > 0} \rightarrow \rho_0 \int_0^1 dk'$ and $\frac{1}{L} \sum_{k \leq k_F} = \frac{1}{L} \sum_{k < 0} \rightarrow \rho_0 \int_{-1}^0 dk$. In Fig. 15 we plot the prefactor c in the expression for the exchange constant $J_{\text{RKKY}} = c 16V^4 / (D^2 U)$ as a function of U/D . In the wideband limit, i.e., for small U/D , c approaches a constant value of $c = 0.616$ irrespective of the value of δ/U . The dependence of c on δ for $U/D \sim 1$ is due to the band-edge effects.

To determine the temperature T_J at which the RKKY interaction becomes fully established, we calculate the cutoff dependent $J_{\text{RKKY}}(E)$, where E is the low-energy cutoff for k and k' integrations, i.e., the integrals over k and k' become $\int_E^1 dk'$ and $\int_{-1}^{-E} dk$. In Fig. 16 we plot the ratio $\xi(E) = J_{\text{RKKY}}(E) / J_{\text{RKKY}}^0$, where $J_{\text{RKKY}}^0 = J_{\text{RKKY}}(E \rightarrow 0)$. The ratio $\xi(E)$ reaches an (arbitrarily chosen) value of 0.9 at $E/U \sim 0.02$. This value of E roughly defines T_J below which the RKKY is fully developed. For small enough V (i.e., Γ), the value of T_J is positioned between T_1^* (free-orbital to local-moment transition temperature) and T_F^* , the temperature of ferromagnetic ordering of spins, given by $T_F^* = J_{\text{RKKY}}^0 / \beta$, where β is a constant of the order one. For larger V , however, $J_{\text{RKKY}}(T)$ does not reach its limiting value at the temperature where the spins start to order. In this case we obtain the ordering temperature T_F numerically as the solution of the implicit equation

$$T_F^* = J_{\text{RKKY}}(T_F^*) / \beta. \tag{A5}$$

An approximate fit to $\xi(E)$ in the wideband limit is $\xi(E) = 1 / (1 + xE/U)$ with $x = 12.2$. We then obtain a solution for T_F^* in closed form:

$$\begin{aligned}
T_F^* &= \frac{\sqrt{1 + 4x/\beta(J_{\text{RKKY}}^0/U)} - 1}{2x/U} \\
&\approx \frac{J_{\text{RKKY}}^0}{\beta} \left[1 - \frac{x}{\beta} \frac{J_{\text{RKKY}}^0}{U} + \mathcal{O}\left(\frac{J_{\text{RKKY}}^0}{U}\right)^2 \right].
\end{aligned} \tag{A6}$$

2. Sixfold symmetric $U_{12} = U$ case

We study the splitting between the singlet, the triplet (same as above), and the ‘‘exciton’’ states $|I=0\rangle = 1/\sqrt{2}(|\uparrow\downarrow, 0\rangle - |0, \uparrow\downarrow\rangle)$ and $|I=1\rangle = 1/\sqrt{2}(|\uparrow\downarrow, 0\rangle + |0, \uparrow\downarrow\rangle)$. Second order corrections are all equal: $E_S^{(2)} = E_T^{(2)} = E_{I=0}^{(2)} = E_{I=1}^{(2)} = -(S_1 + S_2)$ where S_1 and S_2 are the same as in the previously treated $U_{12} = 0$ case. There is again no splitting to second order in V . The fourth order corrections are

$$\begin{aligned}
E_S^{(4)} &= W_S^{\text{ph}} + W_S^{\text{pp}} + W_S^{\text{hh}}, \\
E_T^{(4)} &= W_T^{\text{ph}}, \\
E_{I=0}^{(4)} &= E_T^{(4)}, \\
E_{I=1}^{(4)} &= E_S^{(4)},
\end{aligned} \tag{7}$$

where

$$W_S^{\text{ph}} = 16V^4 \frac{1}{L^2} \sum_{k \leq k_F, k' > k_F} \frac{1}{\epsilon_k - \epsilon_{k'}} \left(\frac{1}{(U - 2\delta + 2\epsilon_k)^2} + \frac{1}{(U + 2\delta - 2\epsilon_{k'})^2} \right),$$

$$\begin{aligned}
 W_T^{\text{ph}} &= 32V^4 \frac{1}{L^2} \sum_{k \leq k_F, k' > k_F} \frac{3U^2 + 6U(\epsilon_k - \epsilon_{k'}) + 4[\delta^2 + \epsilon_k^2 + \epsilon_{k'}^2 - \epsilon_k \epsilon_{k'} - \delta(\epsilon_k + \epsilon_{k'})]}{(U - 2\delta + 2\epsilon_k)^2 (U + 2\delta - 2\epsilon_k)^2 (\epsilon_k - \epsilon_{k'})}, \\
 W_S^{\text{pp}} &= 16V^4 \frac{1}{L^2} \sum_{k'_1 > k_F, k'_2 > k_F} \frac{2(U - 2\delta + \epsilon_{k'_1} + \epsilon_{k'_2})^2}{(U - 2\delta + 2\epsilon_{k'_1})^2 (U - 2\delta + 2\epsilon_{k'_2})^2 (2U - 2\delta + \epsilon_{k'_1} + \epsilon_{k'_2})}, \\
 W_S^{\text{hh}} &= 16V^4 \frac{1}{L^2} \sum_{k_1 \leq k_F, k_2 \leq k_F} \frac{2(U + 2\delta - \epsilon_{k_1} + \epsilon_{k_2})^2}{(U + 2\delta - 2\epsilon_{k_1})^2 (U + 2\delta - 2\epsilon_{k_2})^2 (2U + 2\delta - \epsilon_{k_1} + \epsilon_{k_2})}.
 \end{aligned} \tag{8}$$

The triplet is degenerate with the $I=0$ state, while the singlet and the $I=1$ state are higher in energy, as determined by performing the integrations (results not shown).

APPENDIX B: SCALING EQUATIONS TO SECOND ORDER IN J

We consider an effective Hamiltonian of the form

$$H = \sum_{k\sigma} \epsilon_k c_{k\sigma}^\dagger c_{k\sigma} + \sum_m E_m X_{mm} + \sum_{mm', kk', \sigma\sigma'} J_{mm'}^{\sigma\sigma'} X_{mm'} c_{k\sigma}^\dagger c_{k'\sigma'}, \tag{B1}$$

where $X_{mm'} = |m\rangle\langle m'|$ are the Hubbard operators and $J_{mm'}^{\sigma\sigma'}$ are generalized exchange constants.

We write²

$$[H_{11} + H_{12}(E - H_{22})^{-1}H_{21} + H_{10}(E - H_{00})^{-1}H_{01}] \psi_1 = E \psi_1, \tag{B2}$$

where subspace 2 corresponds to states with one electron in the upper $|\delta D\rangle$ edge of the conduction band, 0 corresponds to states with one hole in the lower $|\delta D\rangle$ edge of the band, and 1 corresponds to states with no excitations in the edges that are being traced-over. Furthermore, $H_{ij} = P_i H P_j$, where P_i are projectors to the corresponding subspaces i .

To second order, the coupling constants are changed by

$$\begin{aligned}
 \delta J_{mm'}^{\sigma\sigma'} &= \rho_0 |\delta D| \sum_{n\tau} \frac{1}{E - D + \epsilon_k - E_n - H_0} J_{nm}^{\tau\sigma} J_{nm'}^{\sigma\tau} \\
 &\quad - \rho_0 |\delta D| \sum_{n\tau} \frac{1}{E - D - \epsilon_{k'} - E_n - H_0} J_{nm}^{\sigma'\tau} J_{nm'}^{\tau\sigma'}.
 \end{aligned} \tag{B3}$$

We apply these results to the effective low-temperature Kondo Hamiltonian

$$H_{\text{eff}} = H_{\text{band}} + J_1 \mathbf{S} \cdot \mathbf{S}_1 + J_2 \mathbf{S} \cdot \mathbf{S}_2 - J_{\text{RKKY}}^{\text{eff}} (\mathbf{S}_1 \cdot \mathbf{S}_2 - 1/4). \tag{B4}$$

Introducing spin-1 operator \mathbf{S} defined by the following Hubbard operator expressions: $S_z = X_{\uparrow\uparrow} - X_{\downarrow\downarrow}$, $S^+ = \sqrt{2}(X_{\uparrow 0} + X_{0\downarrow})$, and $S^- = (S^+)^\dagger$, we obtain

$$\begin{aligned}
 H &= H_{\text{band}} + \tilde{J} \mathbf{S} \cdot \mathbf{S} + J_{\text{RKKY}}^{\text{eff}} X_{SS} \\
 &\quad + \Delta [s_z (X_{0S} + X_{S0}) + s^+ (X_{1S} - X_{S1}) + s^- (X_{S1} - X_{1S})],
 \end{aligned} \tag{B5}$$

where index S denotes the singlet state and we have

$$\tilde{J} = \frac{J_1 + J_2}{2} = J_0 (1 + \alpha^2) / 2,$$

$$\Delta = \frac{J_1 - J_2}{2} = J_0 (1 - \alpha^2) / 2. \tag{B6}$$

Equations (B3) reduce to two equations for \tilde{J} and Δ

$$\begin{aligned}
 \delta \tilde{J} &= \rho_0 |\delta D| \left[\frac{\tilde{J}^2}{D} + \frac{\Delta^2}{D + J_{\text{RKKY}}^{\text{eff}}} \right], \\
 \delta \Delta &= -2\rho_0 \frac{|\delta D|}{D} \Delta \tilde{J},
 \end{aligned} \tag{B7}$$

from which ensue the following scaling equations:

$$\begin{aligned}
 \frac{d\tilde{J}}{dl} &= -\rho_0 \tilde{J}^2 - \rho_0 \frac{\Delta^2 D}{D + J_{\text{RKKY}}^{\text{eff}}}, \\
 \frac{d\Delta}{dl} &= -2\rho_0 \Delta \tilde{J},
 \end{aligned} \tag{B8}$$

where $l = \log D$. The initial bandwidth D is the effective bandwidth $D_{\text{eff}} = 0.182U$ for the Anderson model and we take $\tilde{J}(l = \log D_{\text{eff}}) = \tilde{J}$ and $\Delta(l = \log D_{\text{eff}}) = \Delta$ with \tilde{J} and Δ taken from Eq. (B6). We integrate the equations numerically until \tilde{J} starts to diverge. The corresponding cutoff D defines the Kondo temperature. The results are shown in Fig. 14. The scaling approach reproduces our NRG results very well.

- ¹P. W. Anderson, *Phys. Rev.* **124**, 41 (1961).
- ²A. C. Hewson, *The Kondo Problem to Heavy-Fermions* (Cambridge University Press, Cambridge, 1993).
- ³K. Vladár and A. Zawadowski, *Phys. Rev. B* **28**, 1564 (1983).
- ⁴V. Madhavan, W. Chen, T. Jamneala, M. Crommie, and N. S. Wingreen, *Science* **280**, 567 (1998).
- ⁵J. Li, W.-D. Schneider, R. Berndt, and B. Delley, *Phys. Rev. Lett.* **80**, 2893 (1998).
- ⁶S. M. Cronenwett, T. H. Oosterkamp, and L. P. Kouwenhoven, *Science* **281**, 540 (1998).
- ⁷V. Madhavan, T. Jamneala, K. Nagaoka, W. Chen, J.-L. Li, S. G. Louie, and M. F. Crommie, *Phys. Rev. B* **66**, 212411 (2002).
- ⁸T. Jamneala, V. Madhavan, and M. F. Crommie, *Phys. Rev. Lett.* **87**, 256804 (2001).
- ⁹P. Wahl, L. Diekhoner, G. Wittich, L. Vitali, M. A. Schneider, and K. Kern, *Phys. Rev. Lett.* **95**, 166601 (2005).
- ¹⁰H. Jeong, A. M. Chang, and M. R. Melloch, *Science* **293**, 2221 (2001).
- ¹¹A. W. Holleitner, R. H. Blick, A. K. Huttel, K. Eberl, and J. P. Kotthaus, *Science* **297**, 70 (2002).
- ¹²W. G. van der Wiel, S. D. Franceschi, J. M. Elzerman, T. Fujisawa, S. Tarucha, and L. P. Kouwenhoven, *Rev. Mod. Phys.* **75**, 1 (2003).
- ¹³N. J. Craig, J. M. Taylor, E. A. Lester, C. M. Marcus, M. P. Hanson, and A. C. Gossard, *Science* **304**, 565 (2004).
- ¹⁴J. C. Chen, A. M. Chang, and M. R. Melloch, *Phys. Rev. Lett.* **92**, 176801 (2004).
- ¹⁵M. A. Ruderman and C. Kittel, *Phys. Rev.* **96**, 99 (1954).
- ¹⁶B. A. Jones and C. M. Varma, *Phys. Rev. Lett.* **58**, 843 (1987).
- ¹⁷B. A. Jones, C. M. Varma, and J. W. Wilkins, *Phys. Rev. Lett.* **61**, 125 (1988).
- ¹⁸B. A. Jones, B. G. Kotliar, and A. J. Millis, *Phys. Rev. B* **39**, 3415 (1989).
- ¹⁹C. Sire, C. M. Varma, and H. R. Krishnamurthy, *Phys. Rev. B* **48**, 13833 (1993).
- ²⁰I. Affleck, A. W. W. Ludwig, and B. A. Jones, *Phys. Rev. B* **52**, 9528 (1995).
- ²¹A. Georges and Y. Meir, *Phys. Rev. Lett.* **82**, 3508 (1999).
- ²²W. Izumida and O. Sakai, *Phys. Rev. B* **62**, 10260 (2000).
- ²³T. Aono and M. Eto, *Phys. Rev. B* **64**, 073307 (2001).
- ²⁴D. Boese, W. Hofstetter, and H. Schoeller, *Phys. Rev. B* **66**, 125315 (2002).
- ²⁵R. Lopez, R. Aguado, and G. Platero, *Phys. Rev. Lett.* **89**, 136802 (2002).
- ²⁶C. Jayaprakash, H. R. Krishnamurthy, and J. W. Wilkins, *Phys. Rev. Lett.* **47**, 737 (1981).
- ²⁷J. B. Silva, W. L. C. Lima, W. C. Oliveira, J. L. N. Mello, L. N. Oliveira, and J. W. Wilkins, *Phys. Rev. Lett.* **76**, 275 (1996).
- ²⁸C. A. Paula, M. F. Silva, and L. N. Oliveira, *Phys. Rev. B* **59**, 85 (1999).
- ²⁹P. Simon, R. Lopez, and Y. Oreg, *Phys. Rev. Lett.* **94**, 086602 (2005).
- ³⁰M. G. Vavilov and L. I. Glazman, *Phys. Rev. Lett.* **94**, 086805 (2005).
- ³¹Y. Utsumi, J. Martinek, P. Bruno, and H. Imamura, *Phys. Rev. B* **69**, 155320 (2004).
- ³²R. López, D. Sánchez, M. Lee, M.-S. Choi, P. Simon, and K. Le Hur, *Phys. Rev. B* **71**, 115312 (2005).
- ³³W. Izumida and O. Sakai, *J. Phys. Soc. Jpn.* **74**, 103 (2005).
- ³⁴H. Tamura and L. Glazman, *Phys. Rev. B* **72**, 121308(R) (2005).
- ³⁵S. Sasaki, S. de Franceschi, J. M. Elzerman, W. G. van der Wiel, M. Eto, S. Tarucha, and L. P. Kouwenhoven, *Nature (London)* **405**, 764 (2000).
- ³⁶W. Izumida, O. Sakai, and S. Tarucha, *Phys. Rev. Lett.* **87**, 216803 (2001).
- ³⁷L. I. Glazman and M. E. Raikh, *JETP Lett.* **47**, 452 (1988).
- ³⁸H. R. Krishnamurthy, J. W. Wilkins, and K. G. Wilson, *Phys. Rev. B* **21**, 1003 (1980).
- ³⁹H. R. Krishnamurthy, J. W. Wilkins, and K. G. Wilson, *Phys. Rev. B* **21**, 1044 (1980b).
- ⁴⁰J. R. Schrieffer and P. A. Wolff, *Phys. Rev.* **149**, 491 (1966).
- ⁴¹K. G. Wilson, *Rev. Mod. Phys.* **47**, 773 (1975).
- ⁴²V. L. Campo and L. N. Oliveira, *Phys. Rev. B* **72**, 104432 (2005).
- ⁴³W. C. Oliveira and L. N. Oliveira, *Phys. Rev. B* **49**, 11986 (1994).
- ⁴⁴N. Andrei, K. Furuya, and J. H. Lowenstein, *Rev. Mod. Phys.* **55**, 331 (1983).
- ⁴⁵V. T. Rajan, J. H. Lowenstein, and N. Andrei, *Phys. Rev. Lett.* **49**, 497 (1982).
- ⁴⁶P. D. Sacramento and P. Schlottmann, *Phys. Rev. B* **40**, 431 (1989).
- ⁴⁷P. W. Anderson, *J. Phys. C* **3**, 2436 (1970).
- ⁴⁸P. Mehta, N. Andrei, P. Coleman, L. Borda, and G. Zarand, *Phys. Rev. B* **72**, 014430 (2005).
- ⁴⁹W. Koller, A. C. Hewson, and D. Meyer, *Phys. Rev. B* **72**, 045117 (2005).
- ⁵⁰M. Vojta, R. Bulla, and W. Hofstetter, *Phys. Rev. B* **65**, 140405(R) (2002).
- ⁵¹P. S. Cornaglia and D. R. Grempel, *Phys. Rev. B* **71**, 075305 (2005).
- ⁵²R. Žitko and J. Bonča, *Phys. Rev. B* **73**, 035332 (2006).
- ⁵³W. Hofstetter and H. Schoeller, *Phys. Rev. Lett.* **88**, 016803 (2002).
- ⁵⁴R. Žitko, J. Bonča, A. Ramšak, and T. Rejec, *Phys. Rev. B* **73**, 153307 (2006).
- ⁵⁵O. Entin-Wohlman, A. Aharony, and Y. Levinson, *Phys. Rev. B* **64**, 085332 (2001).
- ⁵⁶A. Fuhrer, T. Ihn, K. Ensslin, W. Wegscheider, and M. Bichler, *Phys. Rev. Lett.* **91**, 206802 (2004).
- ⁵⁷A. Kogan, G. Granger, M. A. Kastner, D. Goldhaber-Gordon, and H. Shtrikman, *Phys. Rev. B* **67**, 113309 (2003).
- ⁵⁸M. Pustilnik and L. I. Glazman, *Phys. Rev. Lett.* **87**, 216601 (2001).
- ⁵⁹M. Pustilnik, L. I. Glazman, and W. Hofstetter, *Phys. Rev. B* **68**, 161303(R) (2003).
- ⁶⁰W. Hofstetter and G. Zarand, *Phys. Rev. B* **69**, 235301 (2004).
- ⁶¹S. Alexander and P. W. Anderson, *Phys. Rev.* **133**, A1594 (1964).
- ⁶²S. Nishimoto, T. Pruschke, and R. M. Noack, *J. Phys.: Condens. Matter* **18**, 981 (2006).
- ⁶³M. R. Galpin, D. E. Logan, and H. R. Krishnamurthy, *Phys. Rev. Lett.* **94**, 186406 (2005).
- ⁶⁴A. Taraphder and P. Coleman, *Phys. Rev. Lett.* **66**, 2814 (1991).
- ⁶⁵L. De Leo and M. Fabrizio, *Phys. Rev. B* **69**, 245114 (2004).
- ⁶⁶L. Borda, G. Zarand, W. Hofstetter, B. I. Halperin, and J. von Delft, *Phys. Rev. Lett.* **90**, 026602 (2003).
- ⁶⁷J. Mravlje, A. Ramšak, and T. Rejec, *Phys. Rev. B* **72**, 121403(R) (2005).
- ⁶⁸J. Koch, M. E. Raikh, and F. von Oppen, *Phys. Rev. Lett.* **96**, 056803 (2006).
- ⁶⁹G. Usaj, P. Lustemberg, and C. A. Balseiro, *Phys. Rev. Lett.* **94**,

- 036803 (2005).
- ⁷⁰A. A. Aligia, Phys. Rev. Lett. **96**, 096804 (2006).
- ⁷¹C.-Y. Lin, A. H. Castro Neto, and B. A. Jones, Phys. Rev. B **71**, 035417 (2005).
- ⁷²G. Chiappe and A. A. Aligia, Phys. Rev. B **66**, 075421 (2002).
- ⁷³G. Chiappe and A. A. Aligia, Phys. Rev. B **70**, 129903(E) (2004).
- ⁷⁴R. M. Fye, Phys. Rev. B **41**, 2490 (1990).
- ⁷⁵Similar comparisons of NRG and BA results were used in studying the two-stage Kondo screening in the two-impurity Kondo model (Ref. [27](#)) to identify the nature of the first and the second Kondo crossover.